

Review

Inkjet Printing: A Viable Technology for Biosensor Fabrication

Arif Hussain ¹, Naseem Abbas ^{2,*} and Ahsan Ali ^{3,*}

¹ Department of Mechanical Convergence Engineering, Hanyang University, Seoul 04763, Korea; enggaskari@gmail.com

² Department of Mechanical Engineering, Sejong University, Seoul 05006, Korea

³ Department of Mechanical Engineering, Gachon University, Seongnam-si 13120, Korea

* Correspondence: naseem.abbas@sejong.ac.kr (N.A.); ahsanali@gachon.ac.kr (A.A.)

Abstract: Printing technology promises a viable solution for the low-cost, rapid, flexible, and mass fabrication of biosensors. Among the vast number of printing techniques, screen printing and inkjet printing have been widely adopted for the fabrication of biosensors. Screen printing provides ease of operation and rapid processing; however, it is bound by the effects of viscous inks, high material waste, and the requirement for masks, to name a few. Inkjet printing, on the other hand, is well suited for mass fabrication that takes advantage of computer-aided design software for pattern modifications. Furthermore, being drop-on-demand, it prevents precious material waste and offers high-resolution patterning. To exploit the features of inkjet printing technology, scientists have been keen to use it for the development of biosensors since 1988. A vast number of fully and partially inkjet-printed biosensors have been developed ever since. This study presents a short introduction on the printing technology used for biosensor fabrication in general, and a brief review of the recent reports related to virus, enzymatic, and non-enzymatic biosensor fabrication, via inkjet printing technology in particular.

Keywords: inkjet printing; biosensors; mass production; virus; enzymatic sensors



Citation: Hussain, A.; Abbas, N.; Ali, A. Inkjet Printing: A Viable Technology for Biosensor Fabrication. *Chemosensors* **2022**, *10*, 103. <https://doi.org/10.3390/chemosensors10030103>

Academic Editors: Boris Lakard and Christos Kokkinos

Received: 30 December 2021

Accepted: 7 March 2022

Published: 9 March 2022

Publisher's Note: MDPI stays neutral with regard to jurisdictional claims in published maps and institutional affiliations.



Copyright: © 2022 by the authors. Licensee MDPI, Basel, Switzerland. This article is an open access article distributed under the terms and conditions of the Creative Commons Attribution (CC BY) license (<https://creativecommons.org/licenses/by/4.0/>).

1. Introduction

Biosensors: The first report of an enzyme electrode (oxygen biosensor) dates back to 1962 [1], and the term biosensor was introduced by Karl Cammann in 1977 [2]. By definition, a biosensor is “a chemical sensing device in which a biologically derived recognition entity is coupled to a transducer, to allow the quantitative development of some complex biochemical parameter” [3,4]. In other words, it is a device that detects an analyte (enzyme, DNA/RNA, tissue, antibodies, antigen, proteins, etc.) by transducing a biological response into an electrical signal. As such, a biosensor contains a sensor (molecular detection system) that interacts with the analyte, and a physiochemical detector (receptor) that transduces the analyte interaction into a quantifiable electrical signal. In general, there are three categories of biosensors: (i) Mass-based biosensors, also known as gravimetric biosensors, work on the principle of change in mass. These are highly sensitive sensors that respond to minimal mass fluctuations and are especially suited for biomolecules that are neither fluorescent nor electroactive [5,6]. (ii) Optical biosensors work on the principle of optical transduction [7], in which bio-recognition elements, such as enzymes, antibodies, proteins, etc., are fed to an optical transducer, which subsequently produces an electrical signal proportionate to the concentration of the measured substance [8,9]. The measurements can be based on fluorescence, luminescence, or color change. (iii) Electrochemical biosensors, as suggested by the name, convert the electroactive analytes into a quantifiable electrical signal through three comprising bio-recognition elements: analyte, transducer, and instrumentation. After recognition of the specific analyte, the electrode, acting as a transducer, detects the generation of ions during the chemical reactions and converts them into electrical current or voltage [10–12]. In simple words, in the case of optical biosensors,

photon measurements of the analytes are collected, while in the case of electrochemical biosensors, electron measurements are collected instead. An electrochemical biosensor is further classified as a potentiometric, amperometric, conductometric, immunosensor magnetic, or optical biosensor based on the transduction mechanism [13]. Compared to the optical and mass-based biosensors, electrochemical sensors offer miniaturization, simple fabrication, and customized readout circuits [14]. A detailed description of the transduction systems and types of biosensors can be found in a recent review article [15].

Biosensors applications: The severe acute respiratory syndrome coronavirus 2 (SARS-CoV-2) has undoubtedly been devastating, causing approximately 5.4 million deaths globally as of 30 December 2021 according to the World Health Organization (WHO). This extremely contagious virus has symptoms similar to the common flu virus [16,17], subsequently making flu patients COVID-19 suspects and requiring highly expensive molecular-precision virus testing for each individual. In light of such an urgent issue, an economic, rapid, and high-precision assay method for remote point-of-care (POC) testing and detection of SARS-CoV-2 was recently developed (Figure 1) [18]. Within 5–15 min of incubation, using DNA concentrations of 3.0 or 30 aM, respectively, a 0.7 aM limit of detection (LOD) was determined, which is equivalent to the performance of a conventional PCR test. Being a POC device, the need for electricity is also removed.

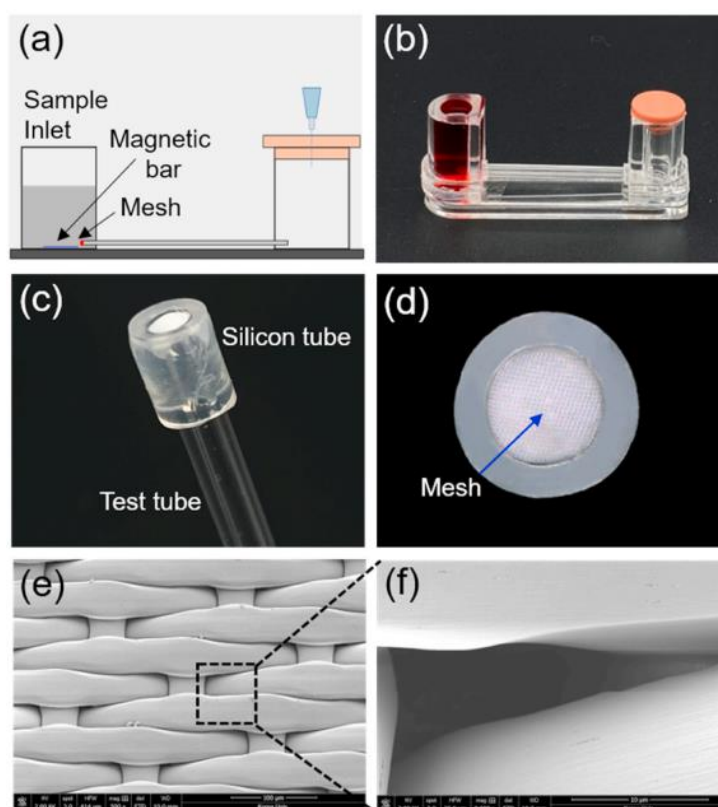


Figure 1. (a) An experimental illustration of a COVID-19 detection microfluidic chip. (b) Three-dimensional (3D) photograph of the experimental apparatus. (c) 3D photograph of a flexible silicon tube bonded to the nylon mesh and glass tube. (d) Front view of the attached nylon mesh with silicon tubing to prevent leaks. (e) SEM image of the nylon mesh. (f) SEM image of a single micro-hole of the nylon mesh. Reprinted with permission from [18].

In other words, the device is capable of being used anywhere and anytime for a rapid, 15 min test for SARS-CoV-2. As such, biosensors can be considered as promising tools for the rapid and easy detection of not just COVID-19, but other viruses as well, for the early diagnosis of infectious diseases [19,20]. Moreover, the ad hoc detection and monitoring of bacterial infections [21,22] can provide convenience for the patients and

improved healthcare in hospitals. Testing food and water contamination is another area where biosensors excel in terms of cost effectiveness and as rapid assay tools [23–25]. In short, biosensors provide portability and the rapid, low-cost, and early diagnosis of pathologies such as cardiac or neurodegenerative diseases, infectious diseases, cancer, fatal viruses, bacterial infections, pregnancy tests, and more, anywhere and anytime. All these conveniences come without the need for specific technical expertise. With the rapid advancement in patterning, microfabrication, and nanofabrication techniques, diverse biosensors production will see a market value of USD 36.7 billion by 2026 [26].

Biosensors Fabrication: Since the fabrication of the first transistor [27], photolithography has been the state-of-the-art choice for microelectronics fabrication due to its high resolution, accuracy, and repeatability [28–30]. The photolithographic technique has been vastly used in silicon integrated circuit (IC) manufacturing, as it can produce extremely small patterns down to the nanometer scale. However, much is left to be desired for such a widely used fabrication technique; for instance, the blanket material deposition and the subsequent photopatterning and etching process in each step cause it to be impractical, expensive, and wasteful for large-area fabrications [31–35]. The use of a high amount of hazardous chemicals renders the process dangerous for indoor industrial employees and the outside environment [36–39]. Moreover, with the increasing trend of flexible electronics [40,41], traditional subtractive fabrication techniques are limited to the use of soft and flexible substrates. The demand for low-cost, rapid, and flexible fabrication methods has led to intensive research activities towards advanced 2D [42] and 3D [43] printing technologies. The drop-on-demand and additive nature of printing technology are its most attractive features. With the rapid development of a variety of printable materials, the area of applications for printing technology is continuously diversifying [44–47]. In addition to general electronic device manufacturing, printing technology has been adopted for the fabrication of biosensors, with the earliest report dating back to as early as 1988 [48], in which an inkjet nozzle was used to deposit an enzyme onto an ion sensitive field effect transistor (ISFET).

Printed Biosensors: The current advanced printing and deposition methods for biosensor fabrication can be classified into two categories; (i) the direct deposition and patterning of material onto the desired substrate, and (ii) the transfer deposition of pre-patterned material onto the substrate. The former technique is achieved via contact (all mask-based techniques) [49,50] and non-contact printing (maskless printing) [15,50,51] technologies, while the latter is achieved by a transfer print after the patterns are brought about via the conventional lithography [52–57] or plasma-modification techniques [58–60]. An immense amount of research has been carried out in the pursuit of fabrication techniques that (i) require a minimum number of fabrication steps, (ii) are flexible in the usage of printable inks, and (iii) are compatible with the appropriate application-based substrates [61]. The reason for such diversity in the printing and deposition techniques is because each technique possesses its own merits and demerits, such that one standalone technique does not suffice for the mass production of all the nano-sized, complicated patterns with high throughput, low cost, and simplicity [62]. For instance, inkjet printing promises mass production with great simplicity and flexibility in terms of ink and substrate selection; however, it is limited in the nozzle sizes required for producing nano-sized features. On the other hand, nanografting techniques are capable of producing nano-sized features, but the technique is not suitable for mass production [63,64]. Although electrostatic inkjet printers and electrohydrodynamic inkjet printers can produce nano-sized spots, both of the printers are limited to conductive inks only [65–67]. Furthermore, photolithography allows for high-resolution patterning at the expense of high cost, requiring multiple steps such as mask preparation, photopatterning, and etching processes [68,69]. Decades of extensive research in the field of printing technologies have led to a major diversification in the number of developed printing techniques. For biosensing fabrication, besides the major contributions of screen printing [70] and inkjet printing [71], other techniques such as 3D printing [72], gravure printing [73], reverse offset printing [74], flexographic printing [75],

e-beam, photo, and probe-based lithographies [76,77], and laser printing [78] have also been studied. The main purpose of the developed printing techniques has been: simplicity, flexibility, miniaturization, high throughput, high accuracy, high resolution, remote applicability, portability, increased data density, and economical fabrication methodologies for mass production. As for now, there is no single printing technology flexible enough to fabricate biosensors with all the above mentioned features, with each technology having certain merits and demerits that have been widely reported [62,79]. Table 1 lists the major printing technologies studied for biosensor fabrication with their merits and limitations. In this short review, we have focused on the recent biosensor fabrication reports for inkjet printing technology in particular. Biosensor fabrication via printing technology is a vast field of study. The purpose here is to provide the readers extended information about the broad category of printing techniques used for biosensor fabrication in a compact manner, then to focus on the review of recent reports where inkjet printing is one of the most promising printing technologies. In Section 2, after a short introduction on inkjet printing technology, we discuss the two major types of inkjet printers, thermal inkjet printers and piezoelectric inkjet printers, including a brief discussion related to the application of inkjet printers in general and in biosensor fabrication. Section 3.1 includes the discussion about virus-based biosensors. In Section 3.2, enzyme-based biosensors are reviewed, while in Section 3.3, the discussion related to the non-enzymatic biosensors has been included.

Table 1. Printing technologies used for biosensors fabrication.

Printing Technology	Biosensors	Merits	References	Limitations
Screen Printing	H ₂ O ₂ detection	Simple, high throughput, economical, robust, rapid, scalable, miniaturization, reliable	[80,81]	Mask-based, contact-based, low production rate compared to roll-to-roll printing, material waste, high material consumption, limited for large scale production
	Glucose sensor		[82]	
	Glucose, glutamate, lactate sensor		[83]	
	pH sensor		[84]	
	Uric Acid sensor		[85]	
	Dopamine detection		[86]	
	SARS-CoV-2		[87,88]	
	MERS-CoV		[89]	
Inkjet Printing	<i>Escherichia coli</i> (<i>E. coli</i>)	Drop-on-demand (DOD), maskless, can create patterns on non-planar surfaces, well-defined patterning, simple, capacity for mass production	[90]	Nozzle clogging, highly specified ink formulation, limited resolution
	Multianalyte (pH, Protein, Glucose) sensor		[91]	
	Ammonia sensor		[92]	
	Pathogen detection		[93]	
	Bienzymatic Glucose biosensor		[94]	
	Calorimetric sensor/ H ₂ O ₂ detection		[95,96]	
	H ₂ O ₂ and glucose detection		[97]	
	Pressure ulcer detection		[98]	
	Wearable biosensor detection system/norovirus detection		[99]	
	HIV-related ssDNA detection		[100]	
	Multiplexed biosensor		[101]	
	Protein detection		[102]	
SARS-CoV-2 detection	[103]			

Table 1. Cont.

Printing Technology	Biosensors	Merits	References	Limitations
3-D Printing	Lactate detection	Ease of design geometries using CAD software and 3D scanner, ability to print complex 3D features	[104]	Limited printing resolution, limited by printable materials
	Multiuse (dopamine, tert-butyl hydroquinone, dipyrone, and diclofenac) sensors		[105]	
	DNA sensing		[106]	
	Dopamine detection		[107]	
	Enzyme biosensor/H ₂ O ₂ detection		[108]	
Gravure Printing	Cadmium sulphide, lead sulphide, D-proline, mouse IgG detection	Roll-to-roll printing, rapid printing, large-area patterning	[73]	High pressure required, low resolution, used for long runs
	Antioxidant Biosensor		[109]	
	Ions, metabolites, heavy metals detection, perspiration monitoring		[110]	
	Glucose sensor		[111]	
Flexographic Printing	Glucose sensor	Roll-to-roll printing, rapid printing, comparatively low pressure required than gravure printing with better resolution, large-area patterning	[112–114]	High pressure required, used for short and medium runs
	Algal toxin detection in water		[115]	
	Human cytomegalovirus (HCMV) detection		[75]	
Microcontact Printing	Protein detection	High resolution down to nm scale, more flexible in terms of ink rheology as compared to inkjet printing, can create patterns on non-planar surfaces	[116]	Transfer printing, requires mask created via photolithography
	Antibody detection		[117,118]	
	Coccidioidomycosis (Valley Fever) detection		[119]	
Laser Printing	Catechol detection/polyphenol biosensor	High spatial resolution, contactless direct-writing technique, no requirement for masks or nozzles, ability to transfer materials both in liquid and solid phase	[120]	Cannot transfer complex multi-component materials, weak bonding between material and substrate, suitable for a few materials only depending on the optical and mechanical properties of the material
	Herbicides detection		[121]	
	Proteins and DNA sensor		[122,123]	
	Heavy metal ions detection		[124]	
	DNA hybridization event detection		[125]	
	Bacteria sensor	[126]		

2. Inkjet Printing

An inkjet printer is comprised of an ink chamber, where the ink is stored, and a channel that connects the ink chamber to the nozzles. The ejection of fluid droplets onto a specified location is controlled digitally. The idea of liquid jet ejection under the influence of gravity was first proposed by Lord Rayleigh in 1878 [127]. A detailed classification of inkjet printers has been reviewed in reference [79]. Among the inkjet printing types, the most dominant and highly developed are thermal and piezoelectric inkjet printers. Both lie under the primary subclass of drop-on-demand (DOD) printers, which also include Electrostatic [128], Acousto [129], Electro hydrodynamic [130], and Valve [131] inkjet printers. The drop-on-demand principle implies that the printer ejects the ink only when required to avoid precious material waste. The advantage of the DOD printer over the continuous inkjet printer is the elimination of the complex droplet-charging, deflection and recycling system that is an essential part of the continuous inkjet printer [79]. In addition, the DOD inkjet printing system promotes the generation of smaller droplet sizes with a higher placement accuracy. We briefly describe the working principles of both the thermal and piezoelectric inkjet printers with the help of graphic illustration, and highlight the limitations and merits of both of the inkjet printing technologies.

Thermal inkjet printer: Thermal inkjet printing relies on the rapid resistive heating of the ink in the ink chamber, which creates a bubble forcing the fluid out of the nozzle. The resistor vaporizes the fluid at around 300–400 °C, subsequently forming a bubble. Within a few microseconds, the bubble collapses, and as a result, the generated pressure decrease retracts the ink flow from the nozzle and simultaneously refills the ink chamber. Figure 2a illustrates the thermal inkjet printing process.

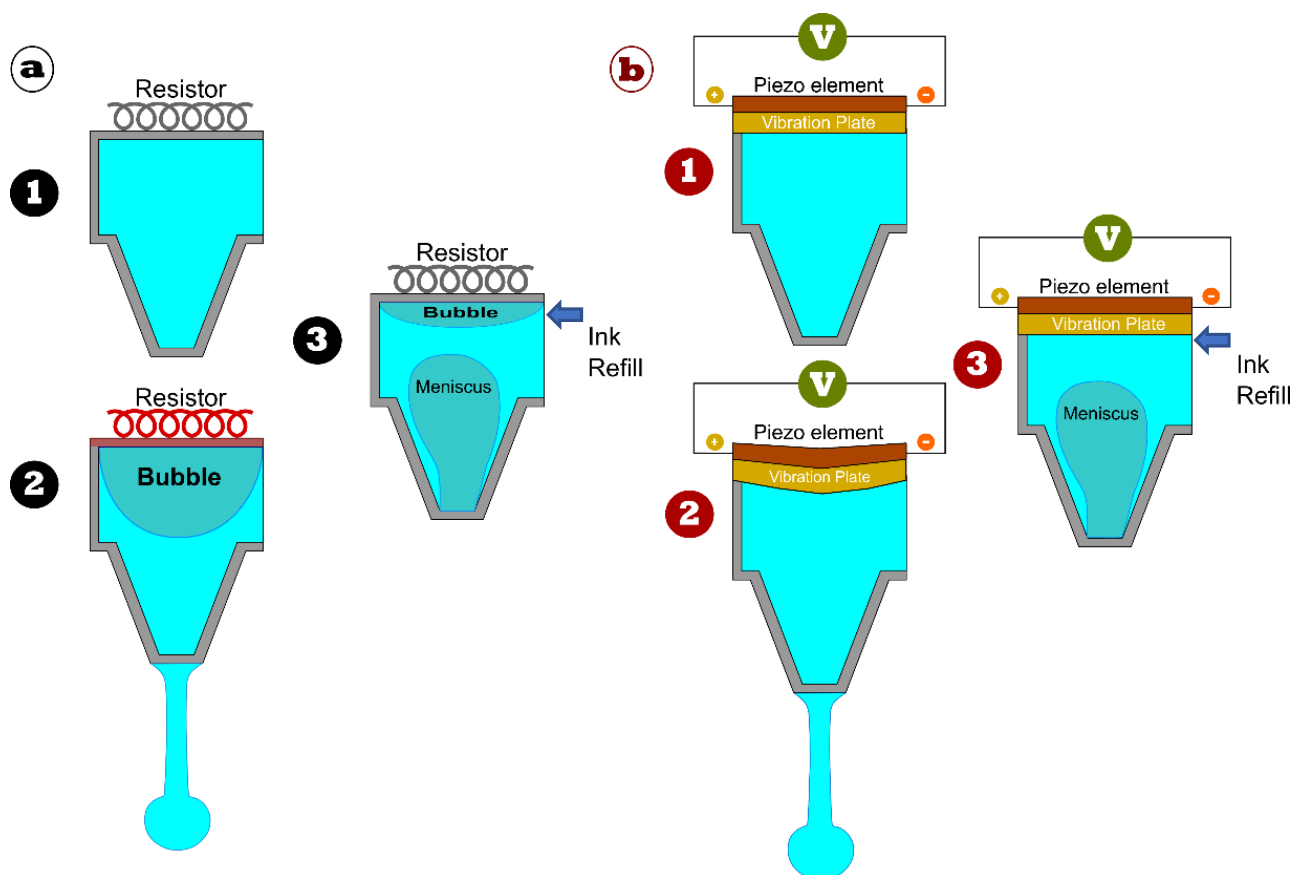


Figure 2. (a) Thermal inkjet printing process: (1) Ink in a stable form in the chamber. (2) The resistor heats up and evaporates the fluid, forming a bubble, and the pressure forces the ink outward from the nozzle cavity. (3) Turning off the resistive heating causes the bubble to subsequently collapse, and a reduction in pressure sucks in the ink both from the nozzle and the ink refill inlet. (b) Piezoelectric printing process (1–3): a similar process as thermal inkjet printing, except here the pressure produced by the piezo element/vibration plate combination stimulates the inkjet and ink refill process.

Piezoelectric inkjet printer: The piezoelectric inkjet printer relies on piezoelectric elements that can deform in shape with the application of voltage. The piezoelectric element is paired with a vibration plate as shown in Figure 2b. The piezoelectric element contracts with the supply of voltage, which then contracts with the vibration plate. This contraction generates an inkjet mechanically unlike the heat generated in the thermal inkjet printing process.

Limitations and merits: Both the thermal and piezoelectric inkjet printers have their limitations and merits. The high temperatures produced in the thermal inkjet printer limit the usability of a wide range of inks [132,133]. For starters, the ink needs to be vaporizable and, at the same time, thermally stable. Reports suggest the thermal degradation of ink materials, such as biological or organic materials, via thermal inkjet printing [134]. However, the thermal degradation of the inks highly depends on the thermal stability of the material used in the inks, which can be application-specific [135]. Based on such limitations, piezoelectric inkjet technology is generally favored over thermal inkjets. However, proper tuning of the ink composition and printing technique can overcome a significant loss in the ink characteristics for thermal inkjet printing, as studied in the references [136–138]. Besides, the thermal inkjet printers operate on simpler mechanisms, offer much more environmentally friendly solvents for inks, and offer 1–1.5 cPs of ink viscosities as compared to 5–10 cP for piezoelectric inkjet technology [134,139,140].

3. Inkjet-Printed Biosensors

Inkjet printers are extremely versatile and have been extensively applied in the direct writing of 2D [42,141] and 3D [43,142] features, especially in the field of printed electronics [143], where nanoparticle fluid suspensions (NPFS) and other nanomaterial inks, such as graphene and carbon nanotube (CNT) inks, are used to print electronic patterns. After the inkjet printers began to be applied to functional materials other than graphics and texts in 1985 [144], inkjet printers slowly started to be used in the field of bioprinting for the fabrication of biosensors in the mid-1990s. The first patented inkjet-printed enzyme-based biosensor was developed in 1988 [48]. Since then, inkjet printing has been extensively used for the high throughput, low-cost, rapid, and simple fabrication of biosensor prototypes, and become a viable technology for the biosensors industry [15,79,145].

3.1. Virus Sensors

The painful sample-collection procedure of and the long waiting time required for traditional PCR testing [146] for COVID-19 diagnosis, in addition to the requirement that it be administered by skilled technicians, have been challenging in the control of the highly contagious virus globally [147]. In such a grave situation, underdeveloped and developing countries found it impossible to develop an easy testing and diagnosis system, especially for the unprivileged population, let alone provide them with proper healthcare. As such, SARS-CoV-2 has been devastating, causing mass fatalities across the globe. To overcome the challenges posed by the COVID-19 pandemic, scientists have been keen to develop point-of-care (PoC) diagnostic devices for the early, rapid, and accurate diagnosis of COVID-19. Recently, a highly conductive 2D material, Tungsten diselenide (WSe_2), was used to develop a highly sensitive WSe_2 -based field-effect transistor for the rapid detection of COVID-19 (Figure 3) [148]. Previously, laser-engraved graphene was used to produce a low-cost and highly sensitive telemedicine platform for the rapid and remote detection of COVID-19 that is able to be mass manufactured [149]. Moreover, the novel characteristics and properties of nanoparticles and nanomaterials have been used to develop biosensors that meet the demands of the rapid, point-of-care, and acute detection of COVID-19 and other viruses [150–152]. Such types of need-based research and development boost innovation by bringing about new technologies, such as standalone printing techniques, for the low-cost, high-throughput, simplistic and mass manufacturing of healthcare devices. Access to rapid diagnostic tools has been one of the necessities in the harsh circumstances of the COVID-19 pandemic, especially in underdeveloped countries and for underrepresented minority groups living in developed countries. Biosensors developed via printed technology have been demonstrated as rapid, low-cost, and reliable diagnostic tools to meet such urgent needs [96,102,153,154].

Recently, Tursunniyaz et al. developed a fully inkjet-printed capacitive immunoassay for the reliable, low-cost, and fast-response diagnosis of SARS-CoV-2 antigen binding, by measuring changes in its capacitance. Unlike the photolithographic fabrication of the capacitive immunoassays [155], the inkjet-printed one presented in this study promises a low fabrication cost that could meet the need for affordable, rapid, and reliable diagnostic kits, especially in resource-limited areas. In [156], a material printer equipped with a 1 pL print head was used to print silver nanoparticles with rectangular coplanar electrodes on the Kapton substrate. To increase conductivity, the printed patterns were sintered at 250 °C for 20 min. The spin-coated polyvinylidene fluoride (PVDF) solution on the electrodes acted as an immobilization layer for antibody adsorption. The fabricated immunoassay projects the simplicity provided by an inkjet printing system, and its potential to be integrated into the manufacturing of point-of-care testing (POTC) devices for the rapid, portable, and onsite diagnosis of highly infectious diseases such as SARS-CoV-2.

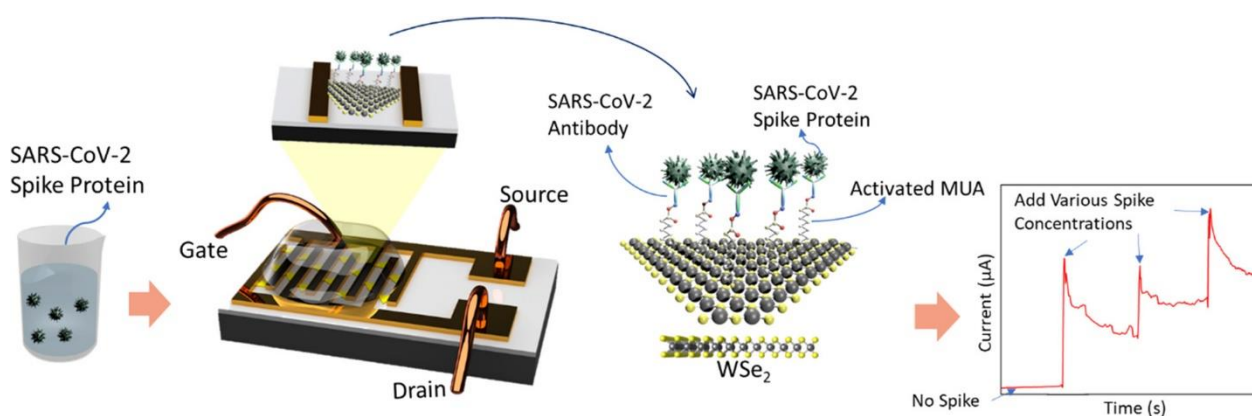


Figure 3. Graphical illustration of the fabrication and working of the monolayer WSe_2 -based FET COVID-19 sensor. The FETs were fabricated via photolithography. Monolayer WSe_2 crystals were functionalized with COVID-19 antibodies (used as a base sensing platform) via 11-mercaptopundecanoic acid (MUA). The MUA was activated with an *n*-hydroxysuccinimide (NHS) and carbodiimide hydrochloride (EDC) solution. The detection of the SARS-CoV-2 spike protein was evaluated by the corresponding effects on the electrical transport properties. Reprinted with permission from [147].

Among the four structural proteins (Spike glycoprotein (S), envelope (E), matrix (M), and nucleocapsid (NC)) of SARS-CoV-2 [157], the spike protein (S) is considered a reliable biomarker for SARS-CoV-2 diagnosis [158,159]. The S protein is further cleaved into two subunits, S1 and S2, by host proteases, among which the S1 subunit is attached to the host cell's receptor for SARS-CoV-2 mediation [160,161]. Besides the electrochemical biosensors developed for SARS-CoV-2 detection [162], printed electrochemical biosensors have also been viable tools for the detection of not only infectious viruses such as MERS-CoV [163], influenza [164], and the like, but also in other PoC sensing applications, such as bacterial infections and pathologies such as cancer and cardiac disease [153]. Very recently, a low-cost, highly sensitive electrochemical biosensor based on a field-effect transistor (CNT-FET) was developed for the accurate detection of SARS-CoV-2 S1 antigens [103]. The biggest advantage of the developed biosensor over the conventional real-time polymerase chain reaction (RT-PCR) testing system is its ability for low cost, reliable, and rapid (2–3 min) detection, overcoming the expensive and laborious 1–2 days of waiting time and the need for a well-equipped laboratory-based testing system. Figure 4 shows the schematic illustration of the CNT-FET biosensor fabrication for the sensing of the SARS-CoV-2 spike protein.

Since the developed biosensor is an electrical immunosensor, it is based on changes in the electrical signal properties that characterize the SARS-CoV-2 S1 antigen binding effect on the sensing area. The source and drain (S-D) electrodes of the CNT-FET were patterned by the photolithography method and lift-off technique. The SWCNT ink that acted as a sensing material was inkjet-printed on the Si/SiO₂ substrate between the active areas of the S-D electrodes and cured on a hot plate at 120 °C in a vacuum chamber for 20 min. The anti-SARS-CoV-2 S1 was immobilized on the printed CNT surface via a 1-pyrenebutanoic acid succinimidyl ester (PBASE) linker through a non-covalent interaction, and the SARS-CoV-2 S1 antigen was subsequently used to characterize the corresponding electrical signal outputs of the biosensor. The presented SWCNT biosensor showed an excellent selectivity specific to the SARS-CoV-2 S1 antigen when tested along with the SARS-CoV-1 S1 and MERS-CoV S1 antigens, such that the biosensor was able to differentiate SARS-CoV-2 S1 and MERS-CoV S1 from their respective antigens. Moreover, the reproducibility and reusability of the biosensor was also successfully demonstrated, indicating the developed biosensor's high potential for low-cost, rapid, simple, and easy-to-use SARS-CoV-2 S1 antigen detection and SARS-CoV-2 virus diagnosis.

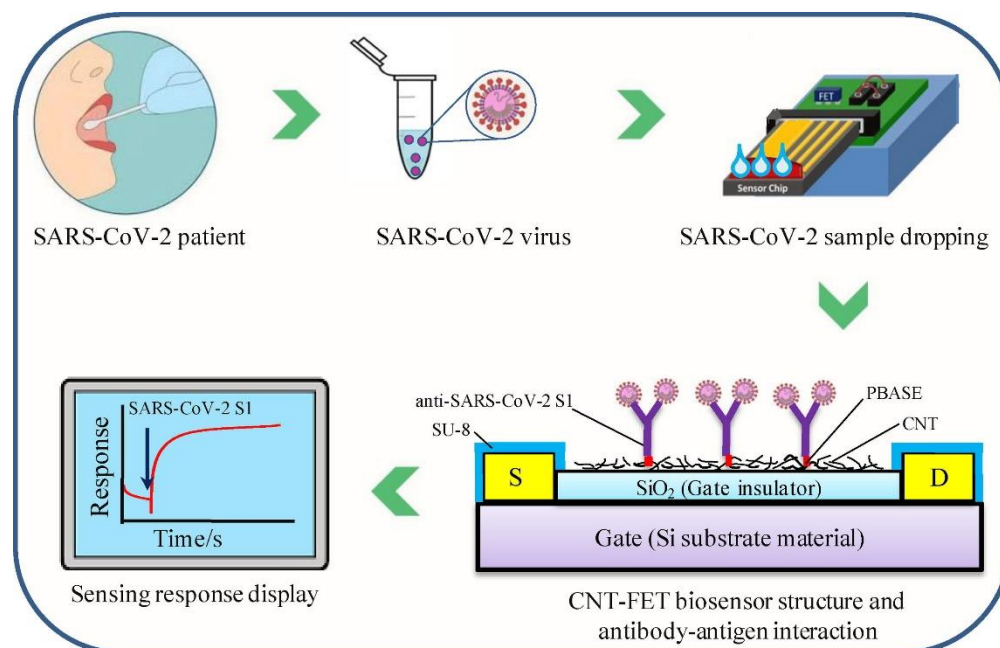


Figure 4. Schematic illustration of the COVID-19 testing steps via CNT-FET biosensor. 1 μL SARS-CoV-2 S1 antigen mixed with 99 μL healthy human saliva to mimic SARS-CoV-2-positive saliva was used as a test sample. The sample was dropped onto the SWCNT surface where anti-SARS-CoV-2 S1 was immobilized via the PBASE linker. SARS-CoV-2 S1 antigen detection was based on the change in S-D current (IDs). The change in the electrical signal characterized the antigen binding effect. Reprinted with permission from [102].

The human norovirus (HuNoV) is a common food-borne illness that causes an estimated 699 million cases of illness, 219,000 deaths, more than USD ~4 billion in direct medical costs, and more than USD ~60 billion in indirect medical cost globally per year [165,166]. One-fifth of acute gastroenteritis is caused by HuNoV worldwide. Although no HuNoV vaccine has been developed so far, as a proof of concept, however, Xiang et al. developed a low-cost, flexible, and wearable inkjet-printed graphene-based FET biosensor to capture norovirus target pathogens from the as-prepared solution [99]. Readers are referred to the original manuscript for the detailed step-by-step inkjet-printed fabrication process of the graphene-based FET biosensor. The biosensor was developed based on intensity changes of the AC signal to avoid high background noise, enabling the detection of biological agents at low concentrations.

More recently, Adly et al. [100] demonstrated an inkjet-printed electrochemical biosensor for the detection of human immunodeficiency virus (HIV)-related single stranded DNA (ssDNA) by immobilizing peptide nucleic acids (PNAs) on inkjet-printed carbon microelectrodes. The device was developed as a proof-of-concept in the development of a microgap device for the amplification of signals of biorecognition events. The redox cycling method [167–169] was used for signal amplification. The redox cycling application is based on the “principle of repeating oxidation and reduction events of redox-active molecules between two closely spaced and independently biased electrodes”. Thus, redox cycling relies on the time taken by a molecule to travel from one electrode to another. If the molecules shuttle rapidly between the oxidizing and the reducing electrodes, strong current amplifications can be obtained. This means that the shorter the distance (micrometer or nanometer) between the electrodes, the more efficient the redox cycling amplification [100]. As such, a separation between the electrodes as low as 500 nm has been successfully obtained via inkjet printing technology with prior substrate adjustments [170]. Adly et al. were able to reduce the distance between two inkjet-printed carbon electrodes down to 1 μm without any prior substrate modification.

3.2. Enzymatic Biosensor

Biosensors are comprised of two main parts: the sensing element, also known as the molecular recognition element (MRE), and the transducing element. The transduction mechanism can be carried out optically, electrically, or by gravimetry, whereas the molecular recognition elements can be antibodies, DNA, enzymes, proteins, or complete cells. One of the earliest reports of an enzyme-based biosensor was in 1967 [171]. An earlier report by Clark and Lyon in 1962 [1] presented an enzyme-based biosensor that used enzyme electrodes, and since then, extensive research has been carried out for the development of enzyme-based biosensors [172,173]. Enzyme-based biosensors can be used to detect glucose, urea, lactose, and xanthine [172]. One of the main concerns of enzyme-based biosensors is their stability and shelf life. If enzyme-containing inks are used for the fabrication of enzyme-based biosensors, for example, with inkjet printers, a major concern is that such inks will have low shelf lives due to the rapid catalytic activity loss of the enzymes in the ink. Techniques to promote better stability and activity, such as employing additives, surface immobilization, enzyme rigidification, and fine-tuned enzyme attachment, have been reported [137,138,174,175]. To address this issue, a recent study [176] developed a technique that caused inkjet-printed enzyme electrodes to retain their sensitivity three months after the ink preparation. To achieve this, the authors formulated a special ink in which, at first, a horseradish peroxidase was covalently immobilized onto silica nanoparticles (SNPs), and then, the SNPs were mixed with an aqueous ink containing single-walled carbon nanotubes (SWCNT). Subsequently, the enzyme electrodes were inkjet-printed with the formulated ink. The immobilization of the biomolecules on the SNPs increased their stability. Figure 5 shows the fabrication steps of the inkjet-printed three-electrode chemical cell. A fully inkjet-printed amperometric hydrogen peroxide biosensor was fabricated to test the performance of the as-prepared enzymatic electrodes.

A study reported by Bai et al. [71] presented yet another inkjet-printed enzyme-based biosensor for point-of-care (POC) analyte detection. In this study, they used multi-walled carbon nanotubes (MWCNT) as enzyme carriers. For enzyme immobilization, a layer-by-layer inkjet printing technique was adopted by cross-linking the ink components between the printed layers. Commercially available disposable screen-printed electrodes, SPEs, on the polyethylene terephthalate (PET) substrates were obtained and treated with a functionalization process, as shown in Figure 6. The schematic shows the layer-by-layer inkjet printing of enzyme ink (layer 1), GLA ink (layer 2), and Nafion ink (layer 3), which were printed to functionalize the working electrode (WE) as a cross-linking and protective ion-selective layer.

The enzyme ink contained MWCNT as enzyme carriers for the enhancement of enzyme loading. The pre-deposited enzyme layer and BSA-glutaraldehyde-enzyme crosslinking gel provided a stable and strong connection between the enzyme and the electrode. Finally, a Nafion layer was printed on top to act as a protective layer for the sensor. Artificial saliva with different concentrations was used for the validity demonstration of the fabricated biosensor. The functionalized SPE with the detection sample was loaded onto a portable potentiostat, where electrochemical experiments were executed and subsequently transmitted to a smartphone app. The results were then displayed on the smartphone screen for the users to interact with. An attractive feature of the developed biosensor was its smartphone integrability, which made it easily usable by a non-expert with the help of a user-friendly Android application. The biosensor offered a wide, linear range with a rapid response time of less than 10s. It allowed for the exchange of the sensing elements and the reagents, rendering it applicable for various types of analyte detection. Finally, a recovery rate of as high as 94% was achieved via artificial saliva testing, suggesting the potential use of the fabricated biosensor system for saliva tests.

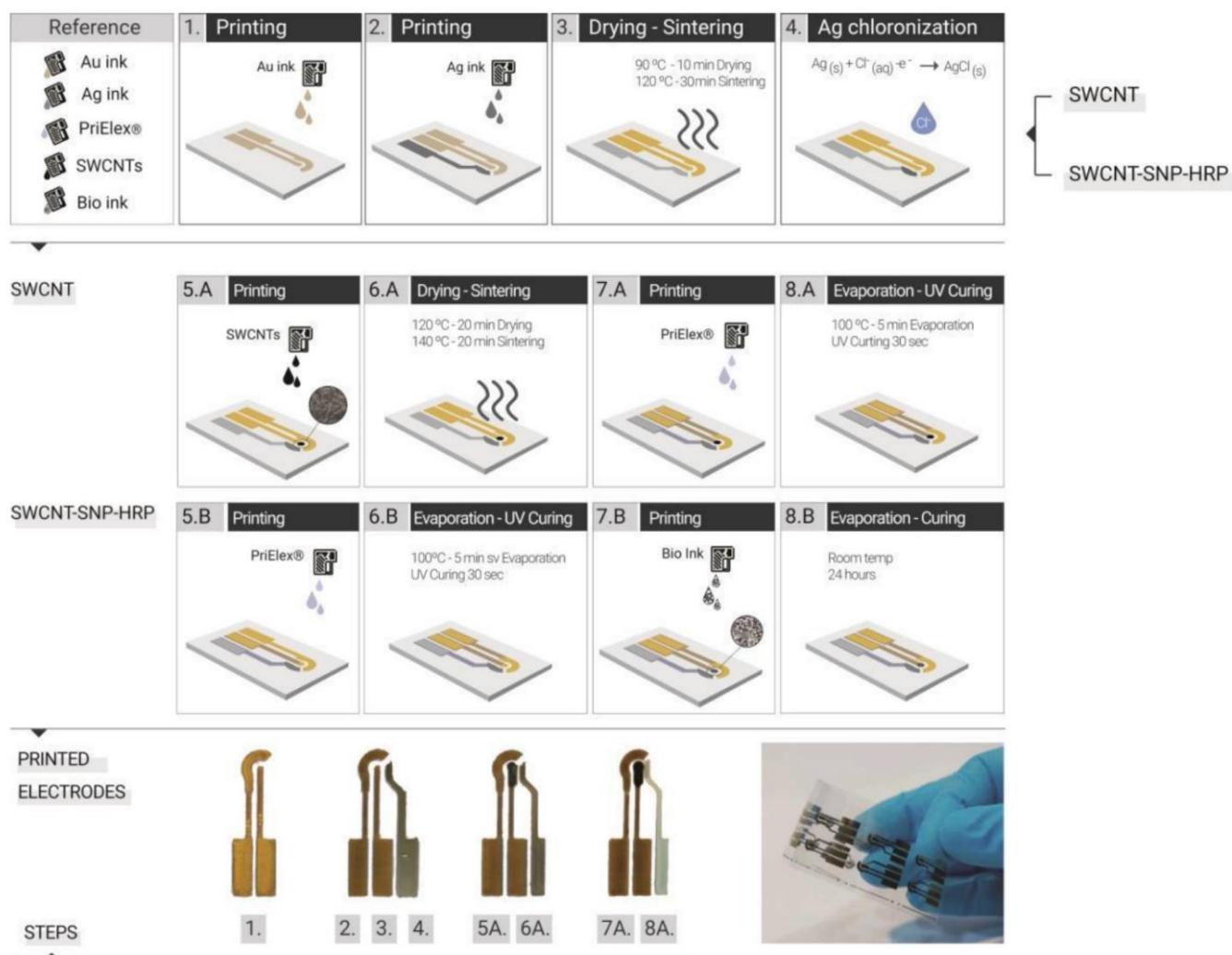


Figure 5. (TOP) Illustration showing the inkjet-printed fabrication steps of the three-electrode electrochemical cell. Polyethylene Terephthalate (PET) was chosen as the substrate. (1–4) Initially, the working electrode (WE) and counter electrode (CE) were printed with Au nanoparticle ink, followed by the printing of the reference electrode (RE) with Ag nanoparticles. After the drying and sintering stage, the Ag electrode was chlorinated for stability purposes. (5.A–8.A) In the next step, a circular area (1 mm dia) was printed on WE with CNT ink, followed by the sintering step. The PriElex[®]SU8 dielectric ink was printed on the conductive paths, followed by hotplate curing. (5.B–8.B) In the final step, following the printing and curing of the dielectric ink, the bio-ink (SWCNT-SNP-HRP) was printed on the active area of WE, followed by room temperature curing to avoid damages and losses in enzymatic activity. (Bottom) Photographic images of the printed electrodes inks and the image of multiple electrodes inkjet printed on flexible PET substrate. Reprinted with permission from [175].

Approximately 422 million people around the world suffer from diabetes mellitus [177], which is projected to rise to 642 million by 2040 [178]. Diabetes mellitus causes blood glucose levels to rise to higher than normal as a result of the body not producing enough insulin (a hormone that controls the amount of glucose in the blood) or simply not responding to the insulin (also called insulin resistance). To avoid such complications, a diabetic patient needs to keep track of their blood glucose levels by performing multiple measurements throughout the day, as blood glucose is an extremely variable parameter. Maintaining glucose levels at an appropriate level is important to prevent or lower the risk for diabetes-induced complications such as heart disease, blindness, kidney failure, and other micro and macrovascular complications [179]. It can also help the patients under-

going insulin therapy inject insulin only when required. Therefore, self-checkup devices that can offer inexpensive, fast, reliable, and convenient pain-free experiences are required. For this purpose, among other glucose-measuring devices, glucose biosensors have been studied and developed for almost 60 years since the first report in 1962 [1].

Sweat-based wearable sensing devices promise several advantages, particularly in healthcare applications [180,181]. On the one hand, wearable sweat sensors are non-invasive and comfortable to use, but on the other hand, these devices can be easily paired with smartphone applications for easy monitoring, even for lay users. Besides being 99% water [182], sweat is composed of cortisol and glucose biomarkers [183,184]. Due to very low concentrations of these biomarkers in sweat, with further dilution for increased sweat flow rates, highly sensitive sensors are required for better precision. Electrochemical sensors, in particular, have been promising for sweat-sensing applications [185,186]. However, current wearable sweat sensors are limited by the lack of available data revealing the effect of sweat volume flow rates [187], the mixture of old and new sweat that reduces sensor reliability [188], and above all, the requirement for expensive and complex fabrication techniques such as photolithography. Very recently, Naik et al. [189] demonstrated the fabrication of a “smart bandage” microfluidic device for single-use cortisol detection and glucose sensing and monitoring. The device was composed of electrochemical sensor-printed graphene and silver inks and an adhesive-based microchannel. The device was integrated with a synthetic skin to understand the perspiration rate for the purposes of validating measurement reliability at various sweating rates. Figure 7 shows the fabrication process of the microfluidic device. The device was specifically designed to project the capability of inkjet-printed methods for inexpensive, customizable, and flexible wearable devices. Besides the glucose monitoring and cortisol measurement, these inkjet-printed devices are true platforms for any type of biosensing device fabrication that is only different in its required design.

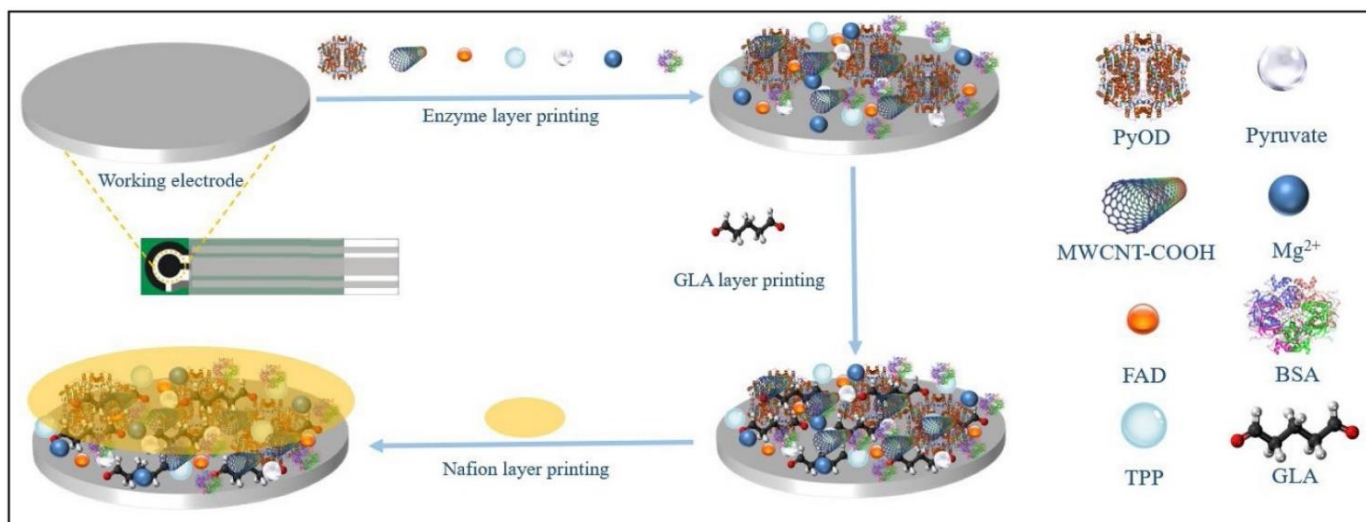


Figure 6. Graphic illustration of the functionalization process of the screen-printed electrodes. Three kinds of inks were sequentially inkjet-printed, layer by layer, on the working electrode. The enzyme layer with biological entities was printed in the first layer, followed by the glutaraldehyde (GLA) layer to form a cross-linking layer. Finally, the Nafion layer was printed to act as a protective layer to encapsulate the sensor. Reprinted with permission from [70].

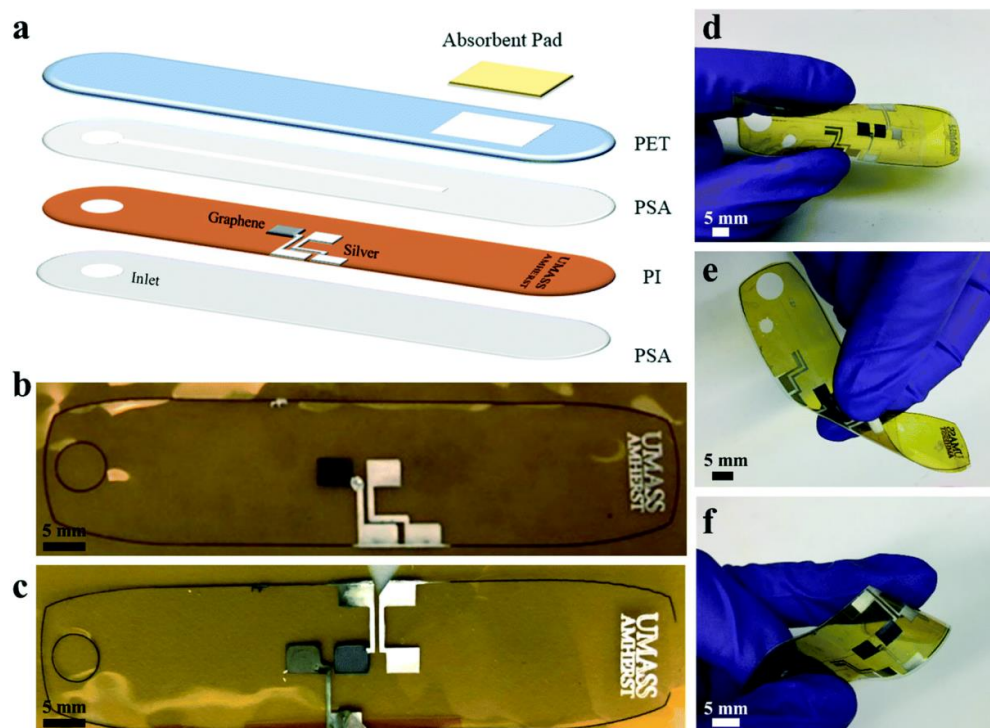


Figure 7. Fabrication of a cortisol detection and glucose-monitoring biosensor. (a) Illustration of laser-cut microfluidic device fabrication and assembly of the electrode and connector layout. Pressure-sensitive adhesive microchannel cutout (1 mm wide) was used between polyimide (PI) and hydrophilic polyethylene terephthalate (PET) (with a SiO₂-based hydrophilic coating) substrates. The absorbent pad was used for constant evaporation of sweat through the device. (b) Inkjet-printed glucose sensor with silver (right) and graphene (left) electrodes. Graphene and silver inks were printed for high-temperature stability. (c) Inkjet-printed chronoamperometric cortisol sensor with silver (right), graphene (middle), and graphene/Au NP (left) electrodes. (d–f) Bending and twisting mechanical deformation demonstration of the assembled cortisol sensor. Reprinted with permission from [189].

3.3. Non-Enzymatic Biosensors

Based on sensing materials, two main categories of biosensors have been developed: enzymatic and non-enzymatic biosensors [190,191]. Although enzymatic biosensors are highly reliable and offer excellent selectivity due to their catalytic behavior [192,193], they are accompanied by certain drawbacks such as high fabrication cost and, more importantly, poor stability of their enzymes. These drawbacks have driven the need for the development of non-enzymatic biosensors. Over the years, extensive studies have been conducted for the development of non-enzymatic biosensors, which have been reviewed elsewhere in detail [194–196]. Electrochemical enzyme-free glucose biosensors have been developed that have higher selectivity, improved sensitivity, and better reproducibility [197–200]. Nanocomposite materials with a high surface area have been exploited for their sensitive detection of glucose via the non-enzymatic electrochemical method [197]. Moreover, nanomaterial-modified glassy carbon electrodes (GCE) have been extensively used for the enzymatic and non-enzymatic electrochemical detection of glucose [197–199,201–203]. As a more convenient alternative in terms of fabrication, and a more ecofriendly approach to the nanomaterial-ink synthesis, paper-based electrochemical and calorimetric sensors have been reported for their low-cost, biodegradable, portable, and highly stable electrochemical analysis of different chemical substances [204,205]. It is as convenient as writing directly with a nano-ink-filled ballpoint pen to fabricate electrochemical sensors on paper substrates [206,207]. Screen printing has also been adopted for the fabrication of both

enzymatic and non-enzymatic electrochemical biosensors on paper substrates, but at the cost of generating a large amount of waste [208,209], which is generally the case with screen-printing technology.

Inkjet printing technology, being drop-on-demand, is a suitable alternative for the fabrication of paper-based electrodes using ecofriendly nanomaterial inks in electrochemical glucose-sensing applications. Recently, an electrochemical, non-enzymatic glucose biosensor was reported, with starch-capped gold nanoparticle (AuNPs) ink inkjet printed on paper substrates to produce paper-based electrodes [210]. The enzyme-free paper-based working electrode was exploited for the analysis of glucose in human blood serum. Figure 8 presents a complete schematic illustration of the AuNPs printed on paper substrates to produce printed paper electrodes (PPE), the working of the PPE, and a cyclic voltammetry representation of the detection of the glucose. The preparation of the active PPE was realized by printing the Au-nano ink on different substrates, such as normal printing paper, bond paper, photo paper, and Whitman filter paper No.1, etc., via a simple desktop inkjet printer. The electrodes were sintered in a hot air oven at 100 °C for 30 min to obtain a minimum resistance of $\sim 0.06 \Omega\text{cm}$. The prepared PPE showed great mechanical stability and flexibility after bending tests were performed at different angles (30°, 90°, and 120°) and the corresponding CV responses were observed. Moreover, the selectivity of the PPE, specifically for the determination of glucose in the blood serum, was also confirmed by introducing interfering species [197,211] such as uric acid, ascorbic acid, and dopamine, along with glucose, in the test sample. No significant change in the detection of glucose in the presence of such compounds was achieved. Overall, a highly selective, simple, ecofriendly, low-cost, and fast methodology was adopted in the fabrication of a robust enzyme-free electrochemical glucose biosensor.

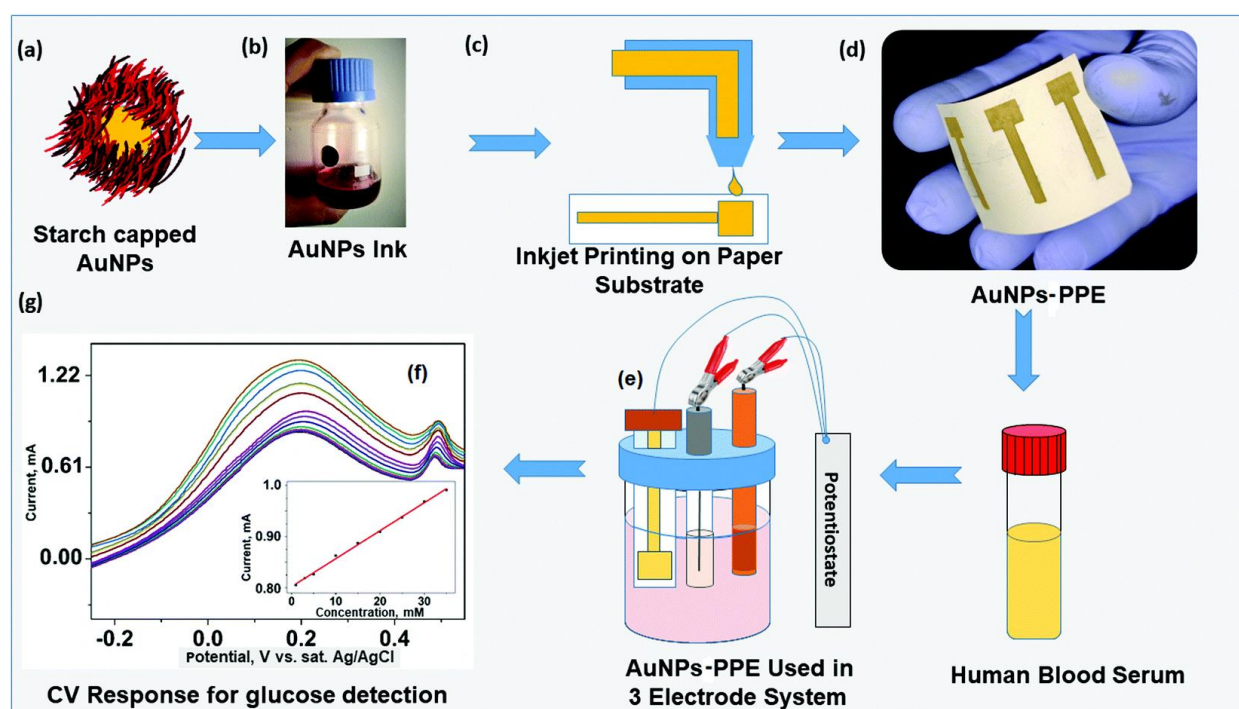


Figure 8. A complete schematic representation of the inkjet-printed paper electrode (PPE) with AuNPs ink, its working, and a cyclic voltammetric (CV) glucose detection chart. (a–d) Starch-encapsulated AuNPs ink preparation with green chemical substances, followed by printing of the electrodes onto the paper substrate. (e) Human blood serum preparation. (f) Testing of the AuNPs-PPE as working electrode. (g) CV responses representing the detection of glucose. Reprinted with permission from [210].

4. Inkjet Printing Technology and the Market Competition

One of the closest competitors to inkjet printing technology is screen printing. Screen printing technology is more widely adopted in biosensor fabrication [212]. However, the biggest disadvantage of screen printing is its subtractive nature, which results in a large amount of precious ink wastage [210]. This, in return, is both costly and environmentally dangerous. Moreover, screen printing is only limited to high-viscosity inks and is a contact-based printing technique. It requires skilled operators and is costly in small-scale production. Another limitation of screen printing is its confinement to flat surfaces, which restricts its use for biosensor fabrication [213]. In comparison, the drop-on-demand nature of inkjet printing technology enables the printing of materials only when required, reducing the wastage of both the electronic and biological inks, while at the same time offering rapid processing, high resolution, and repeatability [214]. Inkjet printing technology allows for the use of a wide variety of inks and for low-temperature printing [215] that supports the use of thermally unstable compounds [216]. The non-contact, maskless, and direct writing capability of inkjet printing enables or allows for (i) combinatorial studies of various devices [217], (ii) CAD data modifications, without the need to change the master template, (iii) a low risk of contamination, (iv) precise spatial control, (v) the use of both solid and flexible substrates, and (vi) the printing of functional materials on 2.5D and 3D surfaces [218]. Inkjet-printing can also be employed as an etch-dispensing process that allows for the use of very small portions of the pre-deposited materials at levels not achievable by its close competitors [219]. One of the major advantages of inkjet printing is the ability to deposit the materials in very small volumes that contain a high loading of nanomaterials or delicate biological materials, at very high speeds.

Besides the screen-printing, other conventional printing techniques such as lithography, flexography, and rotogravure are widely adopted for the mass fabrication of electronic devices. However, each technology possesses its respective drawbacks. Although lithography is a mature technology and offers very high-resolution patterning at high speeds, it requires clean rooms and multistep complex processes, and is costly, specifically for rapid prototyping applications. Flexography offers high-speed and high-quality printing at the expense of long image changing times and costly printing plates. Although even faster and with better printing quality, the rotogravure technology is set back by even longer changeover times and an expensive set up, with printing plates costing as high as 10 times the cost of printing plates required in flexography [220]. Wax-based deposition and cutting plotter are also promising alternatives to screen printing; however, the former uses even more expensive materials while the latter is set back by very low reproducibility [221]. Compared to extrusion printing, stereolithography, laser printing, and microcontact printing, inkjet printing technology is preferable for direct cell printing due to its smaller footprint, high printing resolution, and non-contact nature [222]. 3D printing possesses all the qualities of inkjet printing, but is limited by the availability of printing materials. Readers are referred to [223] for a detailed comparison among inkjet printing, screen printing, gravure printing, and flexographic printing.

Recently, Li et al. [101] reported the fabrication of multiplexed biosensors (Glucose, Lactate, and Triglyceride) via the DOD multinozzle inkjet printing system, printing 96 working electrodes in merely ~5 min. Figure 9 depicts the fabrication steps of the inkjet-printed multiplexed biosensor. Multiplexed biosensors refer to a device which is capable of detecting multiple analytes simultaneously by integrating miniature sensors on a single chip. The study identifies the drawbacks and limitations of traditional photolithography and screen printing for the large-scale fabrication of multiplexed biosensors. It found that photolithography is incompatible with the use of soft materials, while screen printing, being a wasteful process, is more likely to waste the expensive enzyme slurry in a large-scale fabrication process. On the other hand, DOD inkjet printing technology enables the selective printing of different enzymes on the desired areas. As such, a highly sensitive multiplex assay reproducible with good selectivity was fabricated via the DOD inkjet printing system.

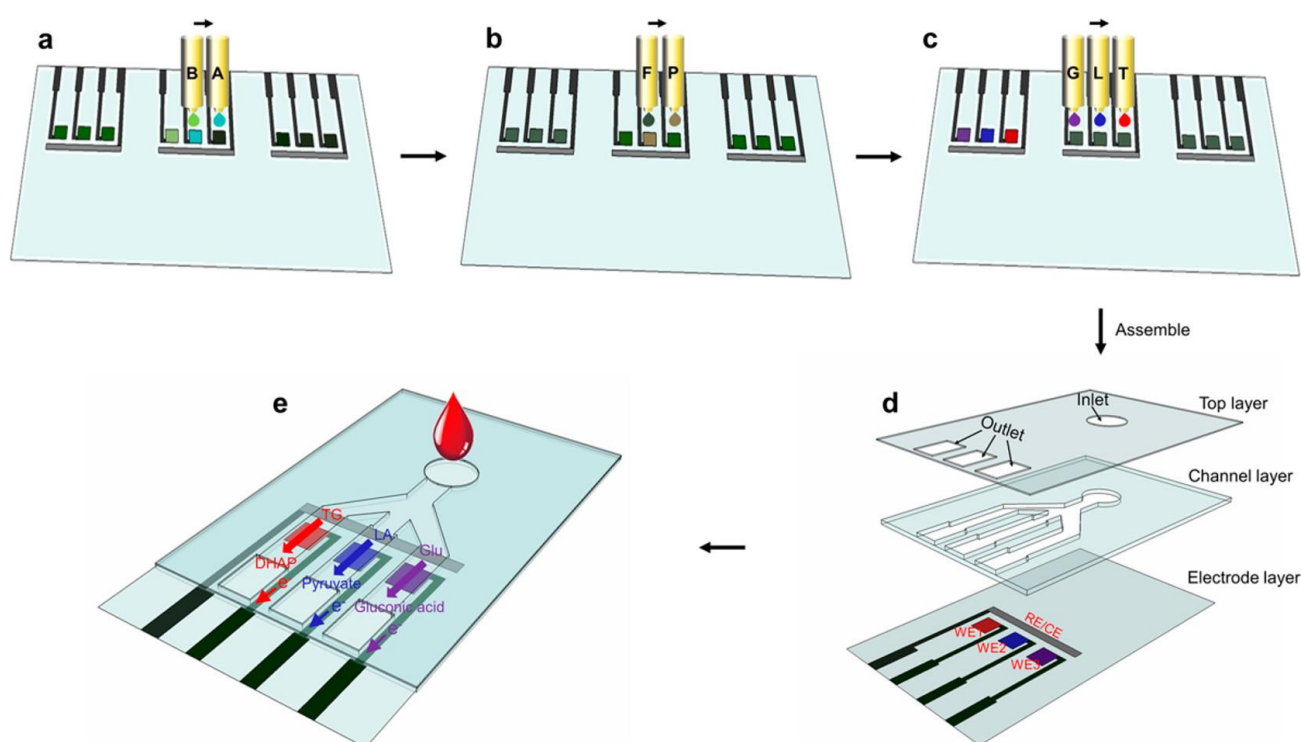


Figure 9. Graphic illustration depicting the fabrication of the inkjet-printed multiplexed biosensor. (a) The conductive polymer polyaniline (PAni) hydrogel was formed on the working electrodes (WE) by sequentially printing precursor solutions A (phytic acid and aniline) and B (ammonium persulfate) on the predefined areas. (b) Chloroplatinic acid (P) and formic acid (F) solutions were printed on the electrode for homogenous high-density loadings of platinum nanoparticles (PtNPs) on the PAni hydrogel film. (c) Enzyme solutions G (glucose oxidase solution, GOx), L (lactic oxidase solution, LOx), and T (mixed solution of l pase/glycerol kinase/L- α -glycerophosphate oxidase, LP/GK/GPO) were sequentially printed onto their designated working electrodes one by one. (d) Finally, the multiplexed biosensor was assembled by integrating the top layer, channel layer, and electrode layer. (e) Schematic of the multiplexed detection of metabolites in human blood with the multiplex assay. Reprinted with permission from [101].

5. Challenges and Limitations

The complete adoption of inkjet printing technology over its competitors has so far been limited due to its limited micrometer-range printing resolution, its nozzle clogging and ink viscosity limitations, and the coffee ring effect. The printing resolution of inkjet printing is decided by the volume of the drop, the drop's impact with the underlying substrate, which is where the rebound effect comes into play, and the spreading or retracting of the ink on the substrate surface, which is governed by the substrate's wettability. The drop production procedure [224] restricts smaller drops, which leaves restructuring the substrate surface before printing as the only option [225]. As the drop impacts the substrate after being jetted from the printer, it may rebound, splash, or spread, depending on whether the surface of the substrate is wetting or non-wetting. Each affects the overall resolution of the printed feature. To help avoid the wetting or de-wetting of the printed droplets, the surface energy of the substrate can be lowered [226]. The rebound of the drop can be avoided by adding small amounts of flexible polymer to the solvent [227]. Lowering the nozzle diameter is another option; however, smaller nozzles clog easier and the machining of such nozzles are expensive. Park et al. used the electrohydrodynamic jetting technique to achieve a feature size of up to 5 μm [228]. Recently, using electrohydrodynamic inkjet printing, Zheng et al. [67] produced hydrogel-based microvascular tissues with a minimum feature size of 30 μm for the hierarchical and branching channels. Ko et al. produced a

1–2 μm line width resolution by a selective laser sintering process following printing [229]. Using the combination of inkjet printing and femtosecond laser sintering, nanoscale metal patterns were produced by Son et al. [230], overcoming the light diffraction limit (see Figure 10).

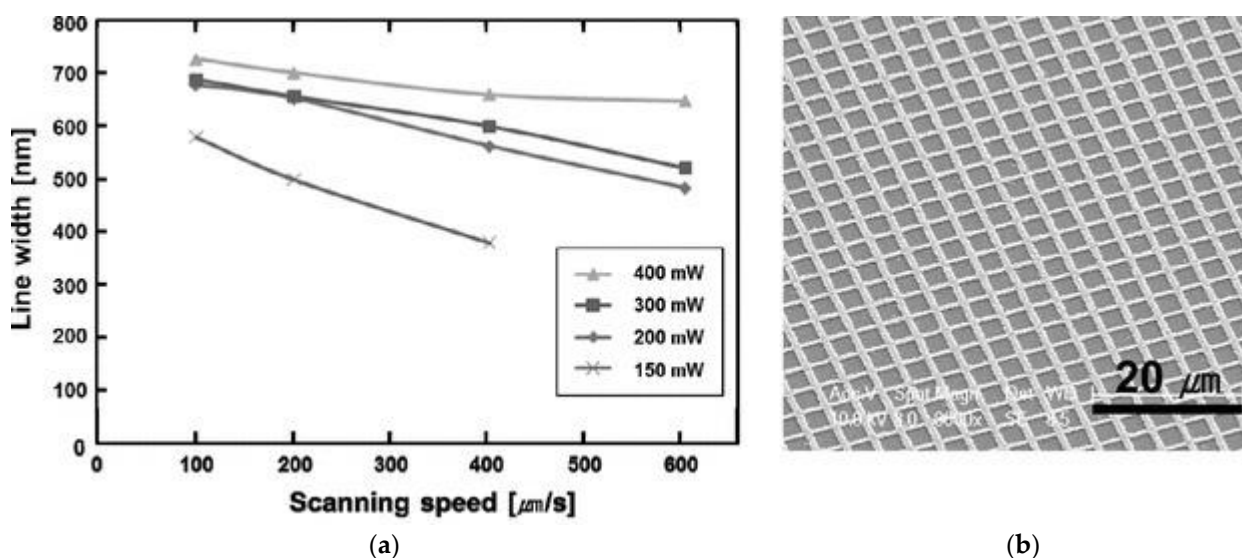


Figure 10. (a) Variation of line width as a function of scanning speed at 150, 200, 300, and 400 mW laser powers (b) SEM image of the mesh pattern of the printed and sintered silver nanoparticles. Reprinted with the permission of [230].

The coffee-ring effect [231] is another fundamental issue with inkjet printing technology, which causes non-uniform film deposition. After the drop's formation on the substrate, the misbalance between the solvent's evaporation and the decrease in the solution volume promotes the radial flow of the residual material from the center to the edges, known as the coffee ring effect [232]. It is possible to print a smooth and uniform line with uniform edges by controlling the drop frequency, temperature, and spacing, as reported by [231]. Recently, a study by Sliz et al. [233] showed both experimentally and through simulation modeling that droplet behavior can be controlled by the substrate's temperature, thus controlling the coffee-ring effect. They showed that up to a critical temperature, an increase in heat transfer causes an increase in the capillary effect, and consequently, an increase in the size of the coffee-ring effect. Beyond the critical temperature, a continuous increase in the temperature tends to diminish the coffee-ring effect. This phenomenon is in agreement with the Leidenfrost effect [234]. Beyond the critical temperature, the coffee-ring effect shape reappears. Although the coffee-ring effect is generally considered an undesirable phenomenon, at the same time, it is exploited for many useful applications [235].

Another major constraint of inkjet printing technology is the limitations caused by ink viscosity. Major competitors such as screen printing and flexography can handle inks with higher viscosity and more solid loadings, while inks with high viscosity and solid contents tend to cause problems such as nozzle clogging and printability [236]. A major constraint also exists for thermal inkjet printers, specifically due to thermally sensitive biological inks. Therefore, piezoelectric inkjet printers are normally preferred over thermal inkjet printers. Nevertheless, due to the advantages of thermal inkjet printers, such as miniaturization [237], special types of inks have been developed to overcome the limitations of thermal inkjet printers for biosensor fabrications [176].

6. Conclusions

Currently, inkjet printing technology is limited by the fine tuning of ink viscosity and surface tension. The requirement for a certain range of viscosity limits the %wt (concent-

tration) of the functional materials in the ink, sometimes leading to the required amount of deposition being obtained only after multiple printing cycles. Since this limitation lies in a domain of ink development specific to inkjet printing, extensive research has been undergoing to overcome all sorts of application-specific limitations. As a result, we have constantly witnessed the compatibility of inkjet printing with all types of nanoparticles, nanomaterials, and biological inks that have been developed throughout the years. Moreover, the resolution limitation of inkjet printing systems has also improved significantly since their early developmental stages. The main motivations behind using inkjet printing technology are that it offers simplicity, versatility (application to a vast variety of fields), cost effectiveness, compactness, ease of operation, integrability with CAD software for rapid design modifications, low material waste, and production speed, to name a few. As such, its usability is widely spread across printed flexible, stretchable, and wearable electronics, biosensors, monitoring sensors, etc. Efforts are being made to develop inkjet-printed organic transistors; however, this is currently limited by their low charge carrier mobility, high operating voltage, short lifetime, and very slow switching speeds. Nevertheless, it offers large-area scalability, compatibility with soft substrates, and high printing speeds. Hence, there is still a long way until inkjet printers can be used as a standalone technology for microfabrication and can be exploited at their full potential. Particularly, the majority of the proposed inkjet-printed biosensing devices are, as of yet, proof of concept prototypes, and do not necessarily guarantee an economical manufacturing cost, device sensitivity, or reliability, as compared to the already state-of-the-art industrial microfabrication techniques. Therefore, further research is required for the development of compatible inks, substrates, printing resolutions, and speeds, as well as more effective miniaturization techniques, for inkjet printers to be competitive in the disposable electronic manufacturing market.

Author Contributions: Writing—original draft, investigation, methodology, A.H.; conceptualization, supervision, N.A.; formal analysis, A.A. All authors have read and agreed to the published version of the manuscript.

Funding: This research received no external funding.

Institutional Review Board Statement: Not applicable.

Informed Consent Statement: Not applicable.

Data Availability Statement: Data is contained within the article.

Acknowledgments: We would like to thank the Higher Education Commission of Pakistan for providing fully funded scholarship to Arif Hussain.

Conflicts of Interest: The authors declare no conflict of interest.

References

1. Clark, L.C.; Lyons, C. Electrode Systems for Continuous Monitoring In Cardiovascular Surgery. *Ann. N. Y. Acad. Sci.* **1962**, *102*, 29–45. [[CrossRef](#)] [[PubMed](#)]
2. Cammann, K. Bio-sensors based on ion-selective electrodes. *Fresenius' Z. Für Anal. Chem.* **1977**, *287*, 1–9. [[CrossRef](#)]
3. Pandey, C.M.; Malhotra, B.D. *Biosensors: Fundamentals and Applications*; Sensors and Actuators B, Smithers Rapra Shawbury: Shrewsbury, UK, 2019; Volume 4, pp. 197–206.
4. Reddy, S.M.; Higson, S.P.J.; Vadgama, P.M. Enzyme and other biosensors: Evolution of a technology. *Eng. Sci. Educ. J.* **1994**, *3*, 41–48. [[CrossRef](#)]
5. Afzal, A.; Mujahid, A.; Schirhagl, R.; Bajwa, S.Z.; Latif, U.; Feroz, S. Gravimetric viral diagnostics: QCM based biosensors for early detection of viruses. *Chemosensors* **2017**, *5*, 7. [[CrossRef](#)]
6. Nolan, P.; Auer, S.; Spehar, A.; Oplatowska-Stachowiak, M.; Campbell, K. Evaluation of Mass Sensitive Micro-Array biosensors for their feasibility in multiplex detection of low molecular weight toxins using mycotoxins as model compounds. *Talanta* **2021**, *222*, 121521. [[CrossRef](#)]
7. Mack, N.H.; Wackerly, J.W.; Malyarchuk, V.; Rogers, J.A.; Moore, J.S.; Nuzzo, R.G. Optical transduction of chemical forces. *Nano Lett.* **2007**, *7*, 733–737. [[CrossRef](#)]
8. Damborský, P.; Švitel, J.; Katrlík, J. Optical biosensors. *Essays Biochem.* **2016**, *60*, 91–100. [[CrossRef](#)]
9. Singh, A.; Kumar, V. Recent advances in synthetic biology-enabled and natural whole-cell optical biosensing of heavy metals. *Anal. Bioanal. Chem.* **2021**, *413*, 73–82. [[CrossRef](#)]

10. Ambaye, A.D.; Kefeni, K.K.; Mishra, S.B.; Nxumalo, E.N.; Ntsendwana, B. Recent developments in nanotechnology-based printing electrode systems for electrochemical sensors. *Talanta* **2021**, *255*, 121951. [[CrossRef](#)]
11. Elbadawi, M.; Ong, J.J.; Pollard, T.D.; Gaisford, S.; Basit, A.W. Additive Manufacturable Materials for Electrochemical Biosensor Electrodes. *Adv. Funct. Mater.* **2021**, *31*, 2006407. [[CrossRef](#)]
12. Li, H.; Liu, X.; Li, L.; Mu, X.; Genov, R.; Mason, A.J. CMOS electrochemical instrumentation for biosensor microsystems: A review. *Sensors* **2017**, *17*, 74. [[CrossRef](#)] [[PubMed](#)]
13. Stradiotto, N.R.; Yamanaka, H.; Zanoni, M.V.B. Electrochemical sensors: A powerful tool in analytical chemistry. *J. Braz. Chem. Soc.* **2003**, *14*, 159–173. [[CrossRef](#)]
14. Putnin, T.; Jumpathong, W.; Laocharoensuk, R.; Jakmunee, J.; Ounnunkad, K. A sensitive electrochemical immunosensor based on poly(2-aminobenzylamine) film modified screen-printed carbon electrode for label-free detection of human immunoglobulin G. *Artif. Cells Nanomed. Biotechnol.* **2018**, *46*, 1042–1051. [[CrossRef](#)]
15. Hussin, H.; Soim, N.; Wan Muhamad Hatta, S.F.; Md Rezali, F.A.; Abdul Wahab, Y. Review—Recent Progress in the Diversity of Inkjet-Printed Flexible Sensor Structures in Biomedical Engineering Applications. *J. Electrochem. Soc.* **2021**, *168*, 077508. [[CrossRef](#)]
16. Krishnan, A.; Hamilton, J.P.; Alqahtani, S.A.; Woreta, T.A. A narrative review of coronavirus disease 2019 (COVID-19): Clinical, epidemiological characteristics, and systemic manifestations. *Intern. Emerg. Med.* **2021**, *16*, 815–830. [[CrossRef](#)] [[PubMed](#)]
17. Singhal, T. A Review of Coronavirus Disease-2019 (COVID-19). *Indian J. Pediatr.* **2020**, *87*, 281–286. [[CrossRef](#)] [[PubMed](#)]
18. Kim, H.S.; Abbas, N.; Shin, S. A rapid diagnosis of SARS-CoV-2 using DNA hydrogel formation on microfluidic pores. *Biosens. Bioelectron.* **2021**, *177*, 113005. [[CrossRef](#)]
19. Fani, M.; Zandi, M.; Soltani, S.; Abbasi, S. Future developments in biosensors for field-ready SARS-CoV-2 virus diagnostics. *Biotechnol. Appl. Biochem.* **2021**, *68*, 695–699. [[CrossRef](#)]
20. Maddali, H.; Miles, C.E.; Kohn, J.; O’Carroll, D.M. Optical Biosensors for Virus Detection: Prospects for SARS-CoV-2/COVID-19. *ChemBioChem* **2021**, *22*, 117–1189. [[CrossRef](#)]
21. Nuutila, J.; Hohenthal, U.; Oksi, J.; Jalava-Karvinen, P. Rapid detection of bacterial infection using a novel single-tube, four-colour flow cytometric method: Comparison with PCT and CRP. *EBioMedicine* **2021**, *74*, 103724. [[CrossRef](#)]
22. Munteanu, F.D.; Titoiu, A.M.; Marty, J.L.; Vasilescu, A. Detection of antibiotics and evaluation of antibacterial activity with screen-printed electrodes. *Sensors* **2018**, *18*, 901. [[CrossRef](#)] [[PubMed](#)]
23. Nasrullah, U.; Ishfaq, U.; Qamar, M.; Azam, M.; Zahra Naqvi, W.; Rafeeq, H.; Noor, Z. Review on Biological Techniques, Microbial Food Testing Approaches, Biosensors Principles and Applications. *Sch. Bull.* **2021**, *7*, 82–86. [[CrossRef](#)]
24. Hara, T.O.; Singh, B. Electrochemical Biosensors for Detection of Pesticides and Heavy Metal Toxicants in Water: Recent Trends and Progress. *ACS ES T Water* **2021**, *1*, 462–478. [[CrossRef](#)]
25. Wu, Y.; Wang, C.W.; Wang, D.; Wei, N. A Whole-Cell Biosensor for Point-of-Care Detection of Waterborne Bacterial Pathogens. *ACS Synth. Biol.* **2021**, *10*, 333–344. [[CrossRef](#)] [[PubMed](#)]
26. Haleem, A.; Javaid, M.; Singh, R.P.; Suman, R.; Rab, S. Biosensors applications in medical field: A brief review. *Sens. Int.* **2021**, *2*, 100100. [[CrossRef](#)]
27. Ross, I.M. The invention of the transistor. *Proc. IEEE* **1998**, *86*, 7–28. [[CrossRef](#)]
28. Tran, K.T.M.; Nguyen, T.D. Lithography-based methods to manufacture biomaterials at small scales. *J. Sci. Adv. Mater. Devices* **2017**, *2*, 1–14. [[CrossRef](#)]
29. Cotte, S.; Baraket, A.; Bessueille, F.; Gout, S.; Yaakoubi, N.; Leonard, D.; Errachid, A. *Fabrication of Microelectrodes Using Original “Soft Lithography” Processes*; New Sensors and Processing Chain, Wiley Online Library: Hoboken, NJ, USA, 2014. ISBN 9781119050612.
30. Kokkinos, C.; Economou, A. Recent advances in voltammetric, amperometric and ion-selective (bio)sensors fabricated by microengineering manufacturing approaches. *Curr. Opin. Electrochem.* **2020**, *23*, 21–25. [[CrossRef](#)]
31. Khan, Y.; Thielens, A.; Muin, S.; Ting, J.; Baumbauer, C.; Arias, A.C. A New Frontier of Printed Electronics: Flexible Hybrid Electronics. *Adv. Mater.* **2020**, *32*, 1905279. [[CrossRef](#)]
32. Palavesam, N.; Marin, S.; Hemmetzberger, D.; Landesberger, C.; Bock, K.; Kutter, C. Roll-to-roll processing of film substrates for hybrid integrated flexible electronics. *Flex. Print. Electron.* **2018**, *3*, 014002. [[CrossRef](#)]
33. Lin, S.; Bai, X.; Wang, H.; Wang, H.; Song, J.; Huang, K.; Wang, C.; Wang, N.; Li, B.; Lei, M.; et al. Roll-to-Roll Production of Transparent Silver-Nanofiber-Network Electrodes for Flexible Electrochromic Smart Windows. *Adv. Mater.* **2017**, *29*, 1703238. [[CrossRef](#)] [[PubMed](#)]
34. Koo, H.; Lee, W.; Choi, Y.; Sun, J.; Bak, J.; Noh, J.; Subramanian, V.; Azuma, Y.; Majima, Y.; Cho, G. Scalability of carbon-nanotube-based thin film transistors for flexible electronic devices manufactured using an all roll-To-roll gravure printing system. *Sci. Rep.* **2015**, *5*, 14459. [[CrossRef](#)] [[PubMed](#)]
35. Bucella, S.G.; Luzio, A.; Gann, E.; Thomsen, L.; McNeill, C.R.; Pace, G.; Perinot, A.; Chen, Z.; Facchetti, A.; Caironi, M. Macroscopic and high-throughput printing of aligned nanostructured polymer semiconductors for MHz large-area electronics. *Nat. Commun.* **2015**, *6*, 8394. [[CrossRef](#)] [[PubMed](#)]
36. Huang, S.Z.; Wu, K.Y. Health Risk Assessment of Photoresists Used in an Optoelectronic Semiconductor Factory. *Risk Anal.* **2019**, *39*, 2625–2639. [[CrossRef](#)] [[PubMed](#)]

37. Park, S.H.; Shin, J.A.; Park, H.H.; Yi, G.Y.; Chung, K.J.; Park, H.D.; Kim, K.B.; Lee, S. Exposure to volatile organic compounds and possibility of exposure to by-product volatile organic compounds in photolithography processes in semiconductor manufacturing factories. *Saf. Health Work* **2011**, *2*, 210–217. [[CrossRef](#)]
38. Eom, Y.S.; Hong, J.H.; Lee, S.J.; Lee, E.J.; Cha, J.S.; Lee, D.G.; Bang, S.A. Emission factors of air toxics from semiconductor manufacturing in Korea. *J. Air Waste Manag. Assoc.* **2006**, *56*, 1518–1524. [[CrossRef](#)]
39. Kim, M.H.; Kim, H.; Paek, D. The health impacts of semiconductor production: An epidemiologic review. *Int. J. Occup. Environ. Health* **2014**, *20*, 95–114. [[CrossRef](#)]
40. Kim, J.; Kumar, R.; Bhandokar, A.J.; Wang, J. Advanced Materials for Printed Wearable Electrochemical Devices: A Review. *Adv. Electron. Mater.* **2017**, *3*, 1600260. [[CrossRef](#)]
41. Khan, Y.; Garg, M.; Gui, Q.; Schadt, M.; Gaikwad, A.; Han, D.; Yamamoto, N.A.D.; Hart, P.; Welte, R.; Wilson, W.; et al. Flexible Hybrid Electronics: Direct Interfacing of Soft and Hard Electronics for Wearable Health Monitoring. *Adv. Funct. Mater.* **2016**, *26*, 8764–8775. [[CrossRef](#)]
42. Yan, H.; Chen, Z.; Zheng, Y.; Newman, C.; Quinn, J.R.; Dötz, F.; Kastler, M.; Facchetti, A. A high-mobility electron-transporting polymer for printed transistors. *Nature* **2009**, *457*, 679–689. [[CrossRef](#)]
43. Ursan, I.; Chiu, L.; Pierce, A. Three-dimensional drug printing: A structured review. *J. Am. Pharm. Assoc.* **2013**, *53*, 136–144. [[CrossRef](#)] [[PubMed](#)]
44. Ng, T.N.; Schwartz, D.E.; Lavery, L.L.; Whiting, G.L.; Russo, B.; Krusor, B.; Veres, J.; Bröms, P.; Herlogsson, L.; Alam, N.; et al. Scalable printed electronics: An organic decoder addressing ferroelectric non-volatile memory. *Sci. Rep.* **2012**, *2*, 585. [[CrossRef](#)] [[PubMed](#)]
45. Sekine, C.; Tsubata, Y.; Yamada, T.; Kitano, M.; Doi, S. Recent progress of high performance polymer OLED and OPV materials for organic printed electronics. *Sci. Technol. Adv. Mater.* **2014**, *15*, 034203. [[CrossRef](#)] [[PubMed](#)]
46. Gaikwad, A.M.; Khan, Y.; Ostfeld, A.E.; Pandya, S.; Abraham, S.; Arias, A.C. Identifying orthogonal solvents for solution processed organic transistors. *Org. Electron.* **2016**, *30*, 18–29. [[CrossRef](#)]
47. Chen, S.-P.; Chiu, H.-L.; Wang, P.-H.; Liao, Y.-C. Inkjet Printed Conductive Tracks for Printed Electronics. *ECS J. Solid State Sci. Technol.* **2015**, *4*, P3026–P3033. [[CrossRef](#)]
48. Kimura, J.; Kawana, Y.; Kuriyama, T. An immobilized enzyme membrane fabrication method using an ink jet nozzle. *Biosensors* **1989**, *4*, 41–52. [[CrossRef](#)]
49. Sneek, A.; Ailas, H.; Gao, F.; Leppäniemi, J. Reverse-Offset Printing of Polymer Resist Ink for Micrometer-Level Patterning of Metal and Metal-Oxide Layers. *ACS Appl. Mater. Interfaces* **2021**, *13*, 41782–41792. [[CrossRef](#)]
50. Goh, G.L.; Zhang, H.; Chong, T.H.; Yeong, W.Y. 3D Printing of Multilayered and Multimaterial Electronics: A Review. *Adv. Electron. Mater.* **2021**, *7*, 21004455. [[CrossRef](#)]
51. Goh, G.L.; Agarwala, S.; Yeong, W.Y. Aerosol-Jet-Printed Preferentially Aligned Carbon Nanotube Twin-Lines for Printed Electronics. *ACS Appl. Mater. Interfaces* **2019**, *11*, 43719–43730. [[CrossRef](#)]
52. Kane, R.S.; Takayama, S.; Ostuni, E.; Ingber, D.E.; Whitesides, G.M. Patterning proteins and cells using soft lithography. *Biomater. Silver Jubil. Compend.* **1999**, *20*, 2363–2376. [[CrossRef](#)]
53. Falconnet, D.; Koenig, A.; Assi, F.; Textor, M. A combined photolithographic and molecular-assembly approach to produce functional micropatterns for applications in the biosciences. *Adv. Funct. Mater.* **2004**, *14*, 749–756. [[CrossRef](#)]
54. Park, T.H.; Shuler, M.L. Integration of cell culture and microfabrication technology. *Biotechnol. Prog.* **2003**, *19*, 243–253. [[CrossRef](#)] [[PubMed](#)]
55. Piner, R.D.; Zhu, J.; Xu, F.; Hong, S.; Mirkin, C.A. “Dip-pen” nanolithography. *Science* **1999**, *283*, 661–663. [[CrossRef](#)] [[PubMed](#)]
56. Wilson, D.L.; Martin, R.; Hong, S.; Cronin-Golomb, M.; Mirkin, C.A.; Kaplan, D.L. Surface organization and nanopatterning of collagen by dip-pen nanolithography. *Proc. Natl. Acad. Sci. USA* **2001**, *98*, 13660–13664. [[CrossRef](#)]
57. Rauter, H.; Matyushin, V.; Alguet, Y.; Pittner, F.; Schalkhammer, T. Nanotechnology for smart polymer optical devices. *Macromol. Symp.* **2004**, *217*, 109–134. [[CrossRef](#)]
58. Kampfrath, G.; Hintsche, R. Plasma-Polymerized Thin Films for Enzyme Immobilization in Biosensors. *Anal. Lett.* **1989**, *22*, 2423–2431. [[CrossRef](#)]
59. Hiratsuka, A.; Kojima, K.I.; Muguruma, H.; Lee, K.H.; Suzuki, H.; Karube, I. Electron transfer mediator micro-biosensor fabrication by organic plasma process. *Biosens. Bioelectron.* **2005**, *21*, 957–964. [[CrossRef](#)]
60. Muguruma, H.; Karube, I. Plasma-polymerized films for biosensors. *TrAC—Trends Anal. Chem.* **1999**, *18*, 62–68. [[CrossRef](#)]
61. Stempien, Z.; Kozicki, M.; Pawlak, R.; Korzeniewska, E.; Owczarek, G.; Poscik, A.; Sajna, D. Ammonia gas sensors ink-jet printed on textile substrates. In Proceedings of the IEEE Sensors, Orlando, FL, USA, 30 October–3 November 2016.
62. Gonzalez-Macia, L.; Morrin, A.; Smyth, M.R.; Killard, A.J. Advanced printing and deposition methodologies for the fabrication of biosensors and biodevices. *Analyst* **2010**, *135*, 845–867. [[CrossRef](#)]
63. Schwartz, P.V. Meniscus force nanografting: Nanoscopic patterning of DNA. *Langmuir* **2001**, *17*, 5971–5977. [[CrossRef](#)]
64. Wadu-Mesthrige, K.; Amro, N.A.; Garino, J.C.; Xu, S.; Liu, G.Y. Fabrication of nanometer-sized protein patterns using atomic force microscopy and selective immobilization. *Biophys. J.* **2001**, *80*, 1891–1899. [[CrossRef](#)]
65. Park, J.U.; Lee, J.H.; Paik, U.; Lu, Y.; Rogers, J.A. Nanoscale patterns of oligonucleotides formed by electrohydrodynamic jet printing with applications in biosensing and nanomaterials assembly. *Nano Lett.* **2008**, *8*, 4210–4216. [[CrossRef](#)] [[PubMed](#)]

66. Wang, L.; Kou, R.; Shang, Z.; Weng, Z.; Zhu, C.; Zhong, Y. Corona-Enabled Electrostatic Printing for Ultra-fast Manufacturing of Binder-Free Multifunctional E-Skins. *ACS Appl. Mater. Interfaces* **2021**, *13*, 45966–45976. [[CrossRef](#)] [[PubMed](#)]
67. Zheng, F.; Derby, B.; Wong, J. Fabrication of microvascular constructs using high resolution electrohydrodynamic inkjet printing. *Biofabrication* **2021**, *13*, 035006. [[CrossRef](#)] [[PubMed](#)]
68. Song, J.; Li, Y.; Ke, D.; Wang, D.; Zhang, X.-E. In situ graphene-modified carbon microelectrode array biosensor for biofilm impedance analysis. *Electrochim. Acta* **2021**, *403*, 139570. [[CrossRef](#)]
69. Baracu, A.M.; Dinu Gugoasa, L.A. Review—Recent Advances in Microfabrication, Design and Applications of Amperometric Sensors and Biosensors. *J. Electrochem. Soc.* **2021**, *168*, 037503. [[CrossRef](#)]
70. Zhang, S.; Xie, Y.; Feng, J.; Chu, Z.; Jin, W. Screen-printing of nanocube-based flexible microchips for the precise biosensing of ethanol during fermentation. *AIChE J.* **2021**, *67*, e17142. [[CrossRef](#)]
71. Bai, Y.; Guo, Q.; Xiao, J.; Zheng, M.; Zhang, D.; Yang, J. An inkjet-printed smartphone-supported electrochemical biosensor system for reagentless point-of-care analyte detection. *Sens. Actuators B Chem.* **2021**, *346*, 130447. [[CrossRef](#)]
72. Distler, T.; Boccaccini, A.R. 3D printing of electrically conductive hydrogels for tissue engineering and biosensors—A review. *Acta Biomater.* **2020**, *101*, 1–13. [[CrossRef](#)]
73. Reddy, A.S.G.; Narakathu, B.B.; Atashbar, M.Z.; Rebro, M.; Rebrosova, E.; Joyce, M.K. Gravure printed electrochemical biosensor. *Procedia Eng.* **2011**, *25*, 956–959. [[CrossRef](#)]
74. Nagamine, K.; Tokito, S. Flexible and printed biosensors based on organic TFT devices. *Chem. Gas. Biosens. Internet Things Relat. Appl.* **2019**, 291–306. [[CrossRef](#)]
75. Assaifan, A.K.; Lloyd, J.S.; Samavat, S.; Deganello, D.; Stanton, R.J.; Teng, K.S. Nanotextured Surface on Flexographic Printed ZnO Thin Films for Low-Cost Non-Faradaic Biosensors. *ACS Appl. Mater. Interfaces* **2016**, *8*, 33802–33810. [[CrossRef](#)] [[PubMed](#)]
76. Smolyarova, T.E.; Shanidze, L.V.; Lukyanenko, A.V.; Baron, F.A.; Krasitskaya, V.V.; Kichkailo, A.S.; Tarasov, A.S.; Volkov, N. Talanta Protein biosensor based on Schottky barrier nanowire field effect transistor. *Talanta* **2022**, *239*, 123092. [[CrossRef](#)] [[PubMed](#)]
77. Liu, J.; Jasim, I.; Liu, T.; Huang, J.; Kinzel, E.; Almasri, M. Off-axis microsphere photolithography patterned nanohole array and other structures on an optical fiber tip for glucose sensing. *RSC Adv.* **2021**, *11*, 25912–25920. [[CrossRef](#)]
78. Bordbar, M.M.; Sheini, A.; Hashemi, P.; Hajian, A.; Bagheri, H. Disposable paper-based biosensors for the point-of-care detection of hazardous contaminations—A review. *Biosensors* **2021**, *11*, 316. [[CrossRef](#)]
79. Li, J.; Rossignol, F.; Macdonald, J. Inkjet printing for biosensor fabrication: Combining chemistry and technology for advanced manufacturing. *Lab Chip* **2015**, *15*, 2538. [[CrossRef](#)]
80. Ricci, F.; Amine, A.; Palleschi, G.; Moscone, D. Prussian Blue based screen printed biosensors with improved characteristics of long-term lifetime and pH stability. *Biosens. Bioelectron.* **2002**, *18*, 165–174. [[CrossRef](#)]
81. Sánchez, S.; Pumera, M.; Cabruja, E.; Fàbregas, E. Carbon nanotube/polysulfone composite screen-printed electrochemical enzyme biosensors. *Analyst* **2007**, *132*, 142–147. [[CrossRef](#)]
82. Crouch, E.; Cowell, D.C.; Hoskins, S.; Pittson, R.W.; Hart, J.P. A novel, disposable, screen-printed amperometric biosensor for glucose in serum fabricated using a water-based carbon ink. *Biosens. Bioelectron.* **2005**, *21*, 712–718. [[CrossRef](#)]
83. Jiang, D.; Chu, Z.; Peng, J.; Jin, W. Screen-printed biosensor chips with Prussian blue nanocubes for the detection of physiological analytes. *Sens. Actuators B Chem.* **2016**, *228*, 679–687. [[CrossRef](#)]
84. Rahimi, R.; Ochoa, M.; Parupudi, T.; Zhao, X.; Yazdi, I.K.; Dokmeci, M.R.; Tamayol, A.; Khademhosseini, A.; Ziaie, B. A low-cost flexible pH sensor array for wound assessment. *Sens. Actuators B Chem.* **2016**, *229*, 609–617. [[CrossRef](#)]
85. Shi, W.; Li, J.; Wu, J.; Wei, Q.; Chen, C.; Bao, N.; Yu, C.; Gu, H. An electrochemical biosensor based on multi-wall carbon nanotube-modified screen-printed electrode immobilized by uricase for the detection of salivary uric acid. *Anal. Bioanal. Chem.* **2020**, *412*, 7275–7283. [[CrossRef](#)] [[PubMed](#)]
86. Shen, X.; Ju, F.; Li, G.; Ma, L. Smartphone-based electrochemical potentiostat detection system using PEDOT: PSS/chitosan/graphene modified screen-printed electrodes for dopamine detection. *Sensors* **2020**, *20*, 2781. [[CrossRef](#)] [[PubMed](#)]
87. Fabiani, L.; Saroglia, M.; Galatà, G.; De Santis, R.; Fillo, S.; Luca, V.; Faggioni, G.; D’Amore, N.; Regalbuto, E.; Salvatori, P.; et al. Magnetic beads combined with carbon black-based screen-printed electrodes for COVID-19: A reliable and miniaturized electrochemical immunosensor for SARS-CoV-2 detection in saliva. *Biosens. Bioelectron.* **2021**, *171*, 112686. [[CrossRef](#)] [[PubMed](#)]
88. Pang, S.N.; Lin, Y.L.; Yu, K.J.; Chiou, Y.E.; Leung, W.H.; Weng, W.H. An effective SARS-CoV-2 electrochemical biosensor with modifiable dual probes using a modified screen-printed carbon electrode. *Micromachines* **2021**, *12*, 1171. [[CrossRef](#)]
89. Eissa, S.; Al-Kattan, K.; Zourob, M. Combination of Carbon Nanofiber-Based Electrochemical Biosensor and Cotton Fiber: A Device for the Detection of the Middle-East Respiratory Syndrome Coronavirus. *ACS Omega* **2021**, *6*, 32072. [[CrossRef](#)]
90. Vu, Q.K.; Tran, Q.H.; Vu, N.P.; Anh, T.L.; Le Dang, T.T.; Matteo, T.; Nguyen, T.H.H. A label-free electrochemical biosensor based on screen-printed electrodes modified with gold nanoparticles for quick detection of bacterial pathogens. *Mater. Today Commun.* **2021**, *26*, 101726. [[CrossRef](#)]
91. Abe, K.; Suzuki, K.; Citterio, D. Inkjet-printed microfluidic multianalyte chemical sensing paper. *Anal. Chem.* **2008**, *80*, 6928–6934. [[CrossRef](#)]
92. Crowley, K.; O’Malley, E.; Morrin, A.; Smyth, M.R.; Killard, A.J. An aqueous ammonia sensor based on an inkjet-printed polyaniline nanoparticle-modified electrode. *Analyst* **2008**, *133*, 391–399. [[CrossRef](#)]
93. Abe, K.; Kotera, K.; Suzuki, K.; Citterio, D. Inkjet-printed paperfluidic immuno-chemical sensing device. *Anal. Bioanal. Chem.* **2010**, *398*, 885–893. [[CrossRef](#)]

94. Yun, Y.H.; Lee, B.K.; Choi, J.S.; Kim, S.; Yoo, B.; Kim, Y.S.; Park, K.; Cho, Y.W. A glucose sensor fabricated by piezoelectric inkjet printing of conducting polymers and bienzymes. *Anal. Sci.* **2011**, *27*, 375–379. [[CrossRef](#)] [[PubMed](#)]
95. Maejima, K.; Tomikawa, S.; Suzuki, K.; Citterio, D. Inkjet printing: An integrated and green chemical approach to microfluidic paper-based analytical devices. *RSC Adv.* **2013**, *3*, 9258. [[CrossRef](#)]
96. Soni, A.; Jha, S.K. A paper strip based non-invasive glucose biosensor for salivary analysis. *Biosens. Bioelectron.* **2015**, *67*, 763–768. [[CrossRef](#)] [[PubMed](#)]
97. Weng, B.; Morrin, A.; Shepherd, R.; Crowley, K.; Killard, A.J.; Innis, P.C.; Wallace, G.G. Wholly printed polypyrrole nanoparticle-based biosensors on flexible substrate. *J. Mater. Chem. B* **2014**, *2*, 793. [[CrossRef](#)]
98. Swisher, S.L.; Lin, M.C.; Liao, A.; Leeftang, E.J.; Khan, Y.; Pavinatto, F.J.; Mann, K.; Naujokas, A.; Young, D.; Roy, S.; et al. Impedance sensing device enables early detection of pressure ulcers in vivo. *Nat. Commun.* **2015**, *6*, 6575. [[CrossRef](#)]
99. Xiang, L.; Wang, Z.; Liu, Z.; Weigum, S.E.; Yu, Q.; Chen, M.Y. Inkjet-Printed Flexible Biosensor Based on Graphene Field Effect Transistor. *IEEE Sens. J.* **2016**, *16*, 8359–8364. [[CrossRef](#)]
100. Adly, N.; Feng, L.; Krause, K.J.; Mayer, D.; Yakushenko, A.; Offenhäuser, A.; Wolfrum, B. Flexible Microgap Electrodes by Direct Inkjet Printing for Biosensing Application. *Adv. Biosyst.* **2017**, *1*, 1600016. [[CrossRef](#)]
101. Li, L.; Pan, L.; Ma, Z.; Yan, K.; Cheng, W.; Shi, Y.; Yu, G. All Inkjet-Printed Amperometric Multiplexed Biosensors Based on Nanostructured Conductive Hydrogel Electrodes. *Nano Lett.* **2018**, *18*, 3322–3327. [[CrossRef](#)]
102. Martínez-Domingo, C.; Conti, S.; de la Escosura-Muñiz, A.; Terés, L.; Merkoçi, A.; Ramon, E. Organic-based field effect transistors for protein detection fabricated by inkjet-printing. *Org. Electron.* **2020**, *84*, 105794. [[CrossRef](#)]
103. Zamzami, M.A.; Rabhani, G.; Ahmad, A.; Basalah, A.A.; Al-Sabban, W.H.; Nate Ahn, S.; Choudhry, H. Carbon nanotube field-effect transistor (CNT-FET)-based biosensor for rapid detection of SARS-CoV-2 (COVID-19) surface spike protein S1. *Bioelectrochemistry* **2022**, *143*, 107982. [[CrossRef](#)]
104. Roda, A.; Guardigli, M.; Calabria, D.; Maddalena Calabretta, M.; Cevenini, L.; Michelini, E. A 3D-printed device for a smartphone-based chemiluminescence biosensor for lactate in oral fluid and sweat. *Analyst* **2014**, *139*, 6494–6501. [[CrossRef](#)] [[PubMed](#)]
105. Cardoso, R.M.; Mendonça, D.M.H.; Silva, W.P.; Silva, M.N.T.; Nossol, E.; da Silva, R.A.B.; Richter, E.M.; Muñoz, R.A.A. 3D printing for electroanalysis: From multiuse electrochemical cells to sensors. *Anal. Chim. Acta* **2018**, *1033*, 49–57. [[CrossRef](#)] [[PubMed](#)]
106. Loo, A.H.; Chua, C.K.; Pumera, M. DNA biosensing with 3D printing technology. *Analyst* **2017**, *142*, 279–283. [[CrossRef](#)] [[PubMed](#)]
107. Dos Santos, P.L.; Katic, V.; Loureiro, H.C.; dos Santos, M.F.; dos Santos, D.P.; Formiga, A.L.B.; Bonacin, J.A. Enhanced performance of 3D printed graphene electrodes after electrochemical pre-treatment: Role of exposed graphene sheets. *Sens. Actuators B Chem.* **2019**, *218*, 837–848. [[CrossRef](#)]
108. López Marzo, A.M.; Mayorga-Martinez, C.C.; Pumera, M. 3D-printed graphene direct electron transfer enzyme biosensors. *Biosens. Bioelectron.* **2020**, *151*, 111980. [[CrossRef](#)]
109. Pavinatto, F.J.; Paschoal, C.W.A.; Arias, A.C. Printed and flexible biosensor for antioxidants using interdigitated ink-jetted electrodes and gravure-deposited active layer. *Biosens. Bioelectron.* **2015**, *67*, 553–559. [[CrossRef](#)]
110. Bariya, M.; Shahpar, Z.; Park, H.; Sun, J.; Jung, Y.; Gao, W.; Nyein, H.Y.Y.; Liaw, T.S.; Tai, L.C.; Ngo, Q.P.; et al. Roll-to-Roll Gravure Printed Electrochemical Sensors for Wearable and Medical Devices. *ACS Nano* **2018**, *12*, 6978–6987. [[CrossRef](#)]
111. Kim, K.; Kim, J.; Kim, B.; Ko, S. Fabrication of Microfluidic Structure Based Biosensor Using Roll-to-Roll Gravure Printing. *Int. J. Precis. Eng. Manuf. Green Technol.* **2018**, *5*, 369–374. [[CrossRef](#)]
112. Olkkonen, J.; Lehtinen, K.; Erho, T. Flexographically printed fluidic structures in paper. *Anal. Chem.* **2010**, *82*, 10246–10250. [[CrossRef](#)]
113. Benson, J.; Fung, C.M.; Lloyd, J.S.; Deganello, D.; Smith, N.A.; Teng, K.S. Direct patterning of gold nanoparticles using flexographic printing for biosensing applications. *Nanoscale Res. Lett.* **2015**, *10*, 3596. [[CrossRef](#)]
114. Fung, C.M.; Lloyd, J.S.; Samavat, S.; Deganello, D.; Teng, K.S. Facile fabrication of electrochemical ZnO nanowire glucose biosensor using roll to roll printing technique. *Sens. Actuators B Chem.* **2017**, *247*, 807–813. [[CrossRef](#)]
115. Wang, L.; Zhang, W.; Samavat, S.; Deganello, D.; Teng, K.S. Vertically aligned graphene prepared by photonic annealing for ultrasensitive biosensors. *ACS Appl. Mater. Interfaces* **2020**, *12*, 31. [[CrossRef](#)] [[PubMed](#)]
116. Pattani, V.P.; Li, C.; Desai, T.A.; Vu, T.Q. Microcontact printing of quantum dot bioconjugate arrays for localized capture and detection of biomolecules. *Biomed. Microdevices* **2008**, *10*, 367–374. [[CrossRef](#)] [[PubMed](#)]
117. Angeley, D. Fabrication of an optical-quality linear grating of immunoglobulin G proteins by microcontact printing and demonstration of potential biosensing applications. *Opt. Eng.* **2006**, *45*, 043402. [[CrossRef](#)]
118. Salomon, S.; Leichlé, T.; Dezest, D.; Seichepine, F.; Guillon, S.; Thibault, C.; Vieu, C.; Nicu, L. Arrays of nanoelectromechanical biosensors functionalized by microcontact printing. *Nanotechnology* **2012**, *23*, 495501. [[CrossRef](#)]
119. Tsai, S.M.; Goshia, T.; Chen, Y.C.; Kagiri, A.; Sibal, A.; Chiu, M.H.; Gadre, A.; Tung, V.; Chin, W.C. High-throughput label-free microcontact printing graphene-based biosensor for valley fever. *Colloids Surf. B Biointerfaces* **2018**, *170*, 219–223. [[CrossRef](#)]
120. Touloupakis, E.; Chatzipetrou, M.; Boutopoulos, C.; Gkouzou, A.; Zergioti, I. A polyphenol biosensor realized by laser printing technology. *Sens. Actuators B Chem.* **2014**, *193*, 301–305. [[CrossRef](#)]
121. Touloupakis, E.; Boutopoulos, C.; Buonasera, K.; Zergioti, I.; Giardi, M.T. A photosynthetic biosensor with enhanced electron transfer generation realized by laser printing technology. *Anal. Bioanal. Chem.* **2012**, *402*, 3237–3244. [[CrossRef](#)]

122. Duocastella, M.; Fernández-Pradas, J.M.; Morenza, J.L.; Zafra, D.; Serra, P. Novel laser printing technique for miniaturized biosensors preparation. *Sens. Actuators B Chem.* **2010**, *145*, 596–600. [[CrossRef](#)]
123. Chatzipetrou, M.; Tsekenis, G.; Tsouti, V.; Chatzandroulis, S.; Zergioti, I. Biosensors by means of the laser induced forward transfer technique. *Appl. Surf. Sci.* **2013**, *278*, 250–254. [[CrossRef](#)]
124. Tsekenis, G.; Filippidou, M.K.; Chatzipetrou, M.; Tsouti, V.; Zergioti, I.; Chatzandroulis, S. Heavy metal ion detection using a capacitive micromechanical biosensor array for environmental monitoring. *Sens. Actuators B Chem.* **2015**, *208*, 628–635. [[CrossRef](#)]
125. Skotadis, E.; Voutyras, K.; Chatzipetrou, M.; Tsekenis, G.; Patsiouras, L.; Madianos, L.; Chatzandroulis, S.; Zergioti, I.; Tsoukalas, D. Label-free DNA biosensor based on resistance change of platinum nanoparticles assemblies. *Biosens. Bioelectron.* **2016**, *81*, 388–394. [[CrossRef](#)] [[PubMed](#)]
126. Rabbani, M.; Dalman, Y. Fabrication of biosensors by bacterial printing on different carriers using a laser printer. *Bioprinting* **2020**, *20*, e00099. [[CrossRef](#)]
127. Rayleigh, Lord On the instability of jets. *Proc. Lond. Math. Soc.* **1878**, *s1–10*, 4–13. [[CrossRef](#)]
128. Plog, J.; Jiang, Y.; Pan, Y.; Yarin, A.L. Electrostatically-assisted direct ink writing for additive manufacturing. *Addit. Manuf.* **2021**, *39*, 101644. [[CrossRef](#)]
129. Elrod, S.A.; Hadimioglu, B.; Khuri-Yakub, B.T.; Rawson, E.G.; Richley, E.; Quate, C.F.; Mansour, N.N.; Lundgren, T.S. Nozzleless droplet formation with focused acoustic beams. *J. Appl. Phys.* **1989**, *65*, 3441. [[CrossRef](#)]
130. Khan, A.; Rahman, K.; Ali, S.; Khan, S.; Wang, B.; Bermak, A. Fabrication of circuits by multi-nozzle electrohydrodynamic inkjet printing for soft wearable electronics. *J. Mater. Res.* **2021**, *36*, 3568–3578. [[CrossRef](#)]
131. Mueller, U.; Nyarsik, L.; Horn, M.; Rauth, H.; Przewieslik, T.; Saenger, W.; Lehrach, H.; Eickhoff, H. Development of a technology for automation and miniaturization of protein crystallization. *J. Biotechnol.* **2001**, *85*, 7–14. [[CrossRef](#)]
132. Parashkov, R.; Becker, E.; Riedl, T.; Johannes, H.H.; Kowalsky, W. Large area electronics using printing methods. *Proc. IEEE* **2005**, *93*, 1321–1329. [[CrossRef](#)]
133. Newman, J.D.; Turner, A.P.F.; Marrazza, G. Ink-jet printing for the fabrication of amperometric glucose biosensors. *Anal. Chim. Acta* **1992**, *262*, 13–17. [[CrossRef](#)]
134. Setti, L.; Fraleoni-Morgera, A.; Ballarin, B.; Filippini, A.; Frascaro, D.; Piana, C. An amperometric glucose biosensor prototype fabricated by thermal inkjet printing. *Biosens. Bioelectron.* **2005**, *20*, 2019–2026. [[CrossRef](#)] [[PubMed](#)]
135. Xu, T.; Jin, J.; Gregory, C.; Hickman, J.J.; Boland, T. Inkjet printing of viable mammalian cells. *Biomaterials* **2005**, *26*, 93–99. [[CrossRef](#)] [[PubMed](#)]
136. Setti, L.; Piana, C.; Bonazzi, S.; Ballarin, B.; Frascaro, D.; Fraleoni-Morgera, A.; Giuliani, S. Thermal inkjet technology for the microdeposition of biological molecules as a viable route for the realization of biosensors. *Anal. Lett.* **2004**, *37*, 1559–1570. [[CrossRef](#)]
137. Wang, H.S.; Pan, Q.X.; Wang, G.X. A biosensor based on immobilization of horseradish peroxidase in chitosan matrix cross-linked with glyoxal for amperometric determination of hydrogen peroxide. *Sensors* **2005**, *5*, 266–276. [[CrossRef](#)]
138. Rodrigues, R.C.; Ortiz, C.; Berenguer-Murcia, Á.; Torres, R.; Fernández-Lafuente, R. Modifying enzyme activity and selectivity by immobilization. *Chem. Soc. Rev.* **2013**, *42*, 6290–6307. [[CrossRef](#)] [[PubMed](#)]
139. Nishioka, G.M.; Markey, A.A.; Holloway, C.K. Protein damage in drop-on-demand printers. *J. Am. Chem. Soc.* **2004**, *126*, 16320–16321. [[CrossRef](#)]
140. De Gans, B.J.; Schubert, U.S. Inkjet printing of polymer micro-arrays and libraries: Instrumentation, requirements, and perspectives. *Macromol. Rapid Commun.* **2003**, *24*, 659–666. [[CrossRef](#)]
141. Minemawari, H.; Yamada, T.; Matsui, H.; Tsutsumi, J.Y.; Haas, S.; Chiba, R.; Kumai, R.; Hasegawa, T. Inkjet printing of single-crystal films. *Nature* **2011**, *475*, 364–367. [[CrossRef](#)]
142. Lee, J.Y.; Choi, B.; Wu, B.; Lee, M. Customized biomimetic scaffolds created by indirect three-dimensional printing for tissue engineering. *Biofabrication* **2013**, *5*, 045003. [[CrossRef](#)]
143. Beedasy, V.; Smith, P.J. Printed Electronics as Prepared by Inkjet Printing. *Materials* **2020**, *13*, 704. [[CrossRef](#)]
144. Andresen, P.; Faubel, M.; Haeusler, D.; Kraft, G.; Luelf, H.W.; Skofronick, J.G. Characteristics of a piezoelectric pulsed nozzle beam. *Rev. Sci. Instrum.* **1985**, *56*, 2038. [[CrossRef](#)]
145. Komuro, N.; Takaki, S.; Suzuki, K.; Citterio, D. Inkjet printed (bio)chemical sensing devices. *Anal. Bioanal. Chem.* **2013**, *405*, 5785–5805. [[CrossRef](#)] [[PubMed](#)]
146. Xu, Y.; Xiao, M.; Liu, X.; Xu, S.; Du, T.; Xu, J.; Yang, Q.; Xu, Y.; Han, Y.; Li, T.; et al. Significance of serology testing to assist timely diagnosis of SARS-CoV-2 infections: Implication from a family cluster. *Emerg. Microbes Infect.* **2020**, *9*, 924–927. [[CrossRef](#)] [[PubMed](#)]
147. Cascella, M.; Rajnik, M.; Cuomo, A.; Dulebohn, S.C.; Di Napoli, R. *Features, Evaluation and Treatment Coronavirus (COVID-19) —StatPearls—NCBI Bookshelf*; NCBI: Bethesda, MD, USA, 2020.
148. Fathi-Hafshejani, P.; Azam, N.; Wang, L.; Kuroda, M.A.; Hamilton, M.C.; Hasim, S.; Mahjouri-Samani, M. Two-Dimensional-Material-Based Field-Effect Transistor Biosensor for Detecting COVID-19 Virus (SARS-CoV-2). *ACS Nano* **2021**, *15*, 11461–11469. [[CrossRef](#)] [[PubMed](#)]
149. Torrente-Rodríguez, R.M.; Lukas, H.; Tu, J.; Min, J.; Yang, Y.; Xu, C.; Rossiter, H.B.; Gao, W. SARS-CoV-2 RapidPlex: A Graphene-Based Multiplexed Telemedicine Platform for Rapid and Low-Cost COVID-19 Diagnosis and Monitoring. *Matter* **2020**, *3*, 1981–1998. [[CrossRef](#)]

150. Singh, R.; Hong, S.; Jang, J. Label-free Detection of Influenza Viruses using a Reduced Graphene Oxide-based Electrochemical Immunosensor Integrated with a Microfluidic Platform. *Sci. Rep.* **2017**, *7*, 42771. [[CrossRef](#)]
151. Huang, J.; Xie, Z.; Xie, Z.; Luo, S.; Xie, L.; Huang, L.; Fan, Q.; Zhang, Y.; Wang, S.; Zeng, T. Silver nanoparticles coated graphene electrochemical sensor for the ultrasensitive analysis of avian influenza virus H7. *Anal. Chim. Acta* **2016**, *913*, 121–127. [[CrossRef](#)]
152. Gowri, A.; Ashwin Kumar, N.; Suresh Anand, B.S. Recent advances in nanomaterials based biosensors for point of care (PoC) diagnosis of Covid-19—A minireview. *TrAC-Trends Anal. Chem.* **2021**, *137*, 116205. [[CrossRef](#)]
153. Sardini, E.; Serpelloni, M.; Tonello, S. Printed electrochemical biosensors: Opportunities and metrological challenges. *Biosensors* **2020**, *10*, 166. [[CrossRef](#)]
154. Bihar, E.; Wustoni, S.; Pappa, A.M.; Salama, K.N.; Baran, D.; Inal, S. A fully inkjet-printed disposable glucose sensor on paper. *Npj Flex. Electron.* **2018**, *2*, 30. [[CrossRef](#)]
155. Sanguino, P.; Monteiro, T.; Marques, F.; Dias, C.J.; Igreja, R.; Franco, R. Interdigitated capacitive immunosensors with PVDF immobilization layers. *IEEE Sens. J.* **2014**, *14*, 1260–1265. [[CrossRef](#)]
156. Tursunniyaz, M.; Andrews, J. Printed Capacitive Immunoassay for Detecting SARS-CoV-2 Viral Particles. In Proceedings of the IEEE International Conference on Flexible and Printable Sensors and Systems (FLEPS), Manchester, UK, 20–23 June 2021. [[CrossRef](#)]
157. Wang, H.; Li, X.; Li, T.; Zhang, S.; Wang, L.; Wu, X.; Liu, J. The genetic sequence, origin, and diagnosis of SARS-CoV-2. *Eur. J. Clin. Microbiol. Infect. Dis.* **2020**, *39*, 1629–1635. [[CrossRef](#)] [[PubMed](#)]
158. Yao, H.; Song, Y.; Chen, Y.; Wu, N.; Xu, J.; Sun, C.; Zhang, J.; Weng, T.; Zhang, Z.; Wu, Z.; et al. Molecular Architecture of the SARS-CoV-2 Virus. *Cell* **2020**, *183*, 730–738. [[CrossRef](#)] [[PubMed](#)]
159. Ou, X.; Liu, Y.; Lei, X.; Li, P.; Mi, D.; Ren, L.; Guo, L.; Guo, R.; Chen, T.; Hu, J.; et al. Characterization of spike glycoprotein of SARS-CoV-2 on virus entry and its immune cross-reactivity with SARS-CoV. *Nat. Commun.* **2020**, *11*, 1620. [[CrossRef](#)] [[PubMed](#)]
160. Huang, Y.; Yang, C.; Xu, X.F.; Xu, W.; Liu, S. Structural and functional properties of SARS-CoV-2 spike protein: Potential antiviral drug development for COVID-19. *Acta Pharmacol. Sin.* **2020**, *41*, 1141–1149. [[CrossRef](#)]
161. Walls, A.C.; Park, Y.J.; Tortorici, M.A.; Wall, A.; McGuire, A.T.; Veesler, D. Structure, Function, and Antigenicity of the SARS-CoV-2 Spike Glycoprotein. *Cell* **2020**, *181*, 281–292. [[CrossRef](#)]
162. Shao, W.; Shurin, M.R.; Wheeler, S.E.; He, X.; Star, A. Rapid Detection of SARS-CoV-2 Antigens Using High-Purity Semiconducting Single-Walled Carbon Nanotube-Based Field-Effect Transistors. *ACS Appl. Mater. Interfaces* **2021**, *13*, 10321–10327. [[CrossRef](#)]
163. Layqah, L.A.; Eissa, S. An electrochemical immunosensor for the corona virus associated with the Middle East respiratory syndrome using an array of gold nanoparticle-modified carbon electrodes. *Microchim. Acta* **2019**, *186*, 224. [[CrossRef](#)]
164. Sayhi, M.; Ouerghi, O.; Belgacem, K.; Arbi, M.; Tepeli, Y.; Ghram, A.; Anik, Ü.; Österlund, L.; Laouini, D.; Diouani, M.F. Electrochemical detection of influenza virus H9N2 based on both immunomagnetic extraction and gold catalysis using an immobilization-free screen printed carbon microelectrode. *Biosens. Bioelectron.* **2018**, *107*, 170–177. [[CrossRef](#)]
165. Koo, H.L.; Neill, F.H.; Estes, M.K.; Munoz, F.M.; Cameron, A.; DuPont, H.L.; Atmar, R.L. Noroviruses: The most common pediatric viral enteric pathogen at a large university hospital after introduction of rotavirus vaccination. *J. Pediatric Infect. Dis. Soc.* **2013**, *2*, 57–60. [[CrossRef](#)]
166. Hall, A.J.; Lopman, B.A.; Payne, D.C.; Patel, M.M.; Gastañaduy, P.A.; Vinjé, J.; Parashar, U.D. Norovirus disease in the united states. *Emerg. Infect. Dis.* **2013**, *19*, 1198–1205. [[CrossRef](#)] [[PubMed](#)]
167. Niwa, O.; Xu, Y.; Halsall, H.B.; Heineman, W.R. Small-Volume Voltammetric Detection of 4-Aminophenol with Interdigitated Array Electrodes and Its Application to Electrochemical Enzyme Immunoassay. *Anal. Chem.* **1993**, *65*, 1559–1563. [[CrossRef](#)] [[PubMed](#)]
168. Anderson, L.B.; Reilly, C.N. Thin-layer electrochemistry: Steady-state methods of studying rate processes. *J. Electroanal. Chem.* **1965**, *10*, 295–305. [[CrossRef](#)]
169. Kanno, Y.; Ino, K.; Shiku, H.; Matsue, T. A local redox cycling-based electrochemical chip device with nanocavities for multi-electrochemical evaluation of embryoid bodies. *Lab Chip* **2015**, *23*, 4404–4414. [[CrossRef](#)] [[PubMed](#)]
170. Wang, J.Z.; Zheng, Z.H.; Li, H.W.; Huck, W.T.S.; Siringhaus, H. Dewetting of conducting polymer inkjet droplets on patterned surfaces. *Nat. Mater.* **2004**, *3*, 171–176. [[CrossRef](#)]
171. Updike, S.J.; Hicks, G.P. Reagentless substrate analysis with immobilized enzymes. *Science* **1967**, *158*, 270–272. [[CrossRef](#)]
172. Mohankumar, P.; Ajayan, J.; Mohanraj, T.; Yasodharan, R. Recent developments in biosensors for healthcare and biomedical applications: A review. *Meas. J. Int. Meas. Confed.* **2021**, *167*, 108293. [[CrossRef](#)]
173. Ispas, C.R.; Crivat, G.; Andreescu, S. Review: Recent Developments in Enzyme-Based Biosensors for Biomedical Analysis. *Anal. Lett.* **2012**, *45*, 168–186. [[CrossRef](#)]
174. Hoarau, M.; Badiéyan, S.; Marsh, E.N.G. Immobilized enzymes: Understanding enzyme-surface interactions at the molecular level. *Org. Biomol. Chem.* **2017**, *15*, 9539–9551. [[CrossRef](#)]
175. Cho, I.H.; Kim, D.H.; Park, S. Electrochemical biosensors: Perspective on functional nanomaterials for on-site analysis. *Biomater. Res.* **2020**, *24*, 6. [[CrossRef](#)]
176. Mass, M.; Veiga, L.S.; Garate, O.; Longinotti, G.; Moya, A.; Ramón, E.; Villa, R.; Ybarra, G.; Gabriel, G. Fully inkjet-printed biosensors fabricated with a highly stable ink based on carbon nanotubes and enzyme-functionalized nanoparticles. *Nanomaterials* **2021**, *11*, 1645. [[CrossRef](#)] [[PubMed](#)]
177. Karyakin, A.A. Glucose biosensors for clinical and personal use. *Electrochem. Commun.* **2021**, *125*, 106973. [[CrossRef](#)]

178. Teymourian, H.; Barfidokht, A.; Wang, J. Electrochemical glucose sensors in diabetes management: An updated review (2010–2020). *Chem. Soc. Rev.* **2020**, *49*, 7671. [[CrossRef](#)]
179. Yoo, E.H.; Lee, S.Y. Glucose biosensors: An overview of use in clinical practice. *Sensors* **2010**, *10*, 4558–4576. [[CrossRef](#)]
180. Gao, W.; Emaminejad, S.; Nyein, H.Y.Y.; Challa, S.; Chen, K.; Peck, A.; Fahad, H.M.; Ota, H.; Shiraki, H.; Kiriya, D.; et al. Fully integrated wearable sensor arrays for multiplexed in situ perspiration analysis. *Nature* **2016**, *529*, 509–514. [[CrossRef](#)] [[PubMed](#)]
181. Heikenfeld, J. Technological leap for sweat sensing. *Nature* **2016**, *529*, 475–476. [[CrossRef](#)] [[PubMed](#)]
182. Baker, L.B. Physiology of sweat gland function: The roles of sweating and sweat composition in human health. *Temperature* **2019**, *6*, 211–259. [[CrossRef](#)]
183. Kaushik, A.; Vasudev, A.; Arya, S.K.; Pasha, S.K.; Bhansali, S. Recent advances in cortisol sensing technologies for point-of-care application. *Biosens. Bioelectron.* **2014**, *53*, 499–512. [[CrossRef](#)]
184. Kim, J.; Campbell, A.S.; Wang, J. Wearable non-invasive epidermal glucose sensors: A review. *Talanta* **2018**, *177*, 163–170. [[CrossRef](#)]
185. Bariya, M.; Nyein, H.Y.Y.; Javey, A. Wearable sweat sensors. *Nat. Electron.* **2018**, *1*, 160–171. [[CrossRef](#)]
186. Bandodkar, A.J.; Wang, J. Non-invasive wearable electrochemical sensors: A review. *Trends Biotechnol.* **2014**, *32*, 363–371. [[CrossRef](#)] [[PubMed](#)]
187. Yu, Y.; Nyein, H.Y.Y.; Gao, W.; Javey, A. Flexible Electrochemical Bioelectronics: The Rise of In Situ Bioanalysis. *Adv. Mater.* **2020**, *32*, 1902083. [[CrossRef](#)] [[PubMed](#)]
188. Nyein, H.Y.Y.; Tai, L.C.; Ngo, Q.P.; Chao, M.; Zhang, G.B.; Gao, W.; Bariya, M.; Bullock, J.; Kim, H.; Fahad, H.M.; et al. A Wearable Microfluidic Sensing Patch for Dynamic Sweat Secretion Analysis. *ACS Sensors* **2018**, *3*, 944–952. [[CrossRef](#)] [[PubMed](#)]
189. Naik, A.R.; Zhou, Y.; Dey, A.A.; Arellano, D.L.G.; Okoroanyanwu, U.; Secor, E.B.; Hersam, M.C.; Morse, J.; Rothstein, J.P.; Carter, K.R.; et al. Printed microfluidic sweat sensing platform for cortisol and glucose detection. *Lab Chip* **2022**, *22*, 156–169. [[CrossRef](#)]
190. Ahmed, J.; Rashed, M.A.; Faisal, M.; Harraz, F.A.; Jalalah, M.; Alsareii, S.A. Novel SWCNTs-mesoporous silicon nanocomposite as efficient non-enzymatic glucose biosensor. *Appl. Surf. Sci.* **2021**, *552*, 149477. [[CrossRef](#)]
191. Kim, S.H.; Lee, S.M.; Kim, D.U.; Cui, J.Z.; Kang, S.W. Enzyme-based glucose biosensor using a dye couple system. *Dye. Pigment.* **2001**, *49*, 103–108. [[CrossRef](#)]
192. Hrapovic, S.; Liu, Y.; Male, K.B.; Luong, J.H.T. Electrochemical Biosensing Platforms Using Platinum Nanoparticles and Carbon Nanotubes. *Anal. Chem.* **2004**, *76*, 1083–1088. [[CrossRef](#)]
193. Shi, W.; Ma, Z. Amperometric glucose biosensor based on a triangular silver nanoprisms/chitosan composite film as immobilization matrix. *Biosens. Bioelectron.* **2010**, *26*, 1098–1103. [[CrossRef](#)]
194. Liu, S.; Zeng, W.; Guo, Q.; Li, Y. Metal oxide-based composite for non-enzymatic glucose sensors. *J. Mater. Sci. Mater. Electron.* **2020**, *31*, 16111–16136. [[CrossRef](#)]
195. Si, P.; Huang, Y.; Wang, T.; Ma, J. Nanomaterials for electrochemical non-enzymatic glucose biosensors. *RSC Adv.* **2013**, *3*, 3487–3502. [[CrossRef](#)]
196. Rakesh Kumar, R.K.; Shaikh, M.O.; Chuang, C.H. A review of recent advances in non-enzymatic electrochemical creatinine biosensing. *Anal. Chim. Acta* **2021**, *1183*, 338748. [[CrossRef](#)] [[PubMed](#)]
197. Archana, V.; Xia, Y.; Fang, R.; Gnana Kumar, G. Hierarchical CuO/NiO-Carbon Nanocomposite Derived from Metal Organic Framework on Cello Tape for the Flexible and High Performance Nonenzymatic Electrochemical Glucose Sensors. *ACS Sustain. Chem. Eng.* **2019**, *7*, 6707–6719. [[CrossRef](#)]
198. Chang, G.; Shu, H.; Ji, K.; Oyama, M.; Liu, X.; He, Y. Gold nanoparticles directly modified glassy carbon electrode for non-enzymatic detection of glucose. *Appl. Surf. Sci.* **2014**, *288*, 524–529. [[CrossRef](#)]
199. Tominaga, M.; Shimazoe, T.; Nagashima, M.; Taniguchi, I. Electrocatalytic oxidation of glucose at gold nanoparticle-modified carbon electrodes in alkaline and neutral solutions. *Electrochem. Commun.* **2005**, *7*, 189–193. [[CrossRef](#)]
200. Chen, X.M.; Lin, Z.J.; Chen, D.J.; Jia, T.T.; Cai, Z.M.; Wang, X.R.; Chen, X.; Chen, G.N.; Oyama, M. Nonenzymatic amperometric sensing of glucose by using palladium nanoparticles supported on functional carbon nanotubes. *Biosens. Bioelectron.* **2010**, *25*, 1803–1808. [[CrossRef](#)] [[PubMed](#)]
201. Lee, W.C.; Kim, K.B.; Gurudatt, N.G.; Hussain, K.K.; Choi, C.S.; Park, D.S.; Shim, Y.B. Comparison of enzymatic and non-enzymatic glucose sensors based on hierarchical Au-Ni alloy with conductive polymer. *Biosens. Bioelectron.* **2019**, *130*, 48–54. [[CrossRef](#)] [[PubMed](#)]
202. Zhang, Z.; Liu, H.; Deng, J. A glucose biosensor based on immobilization of glucose oxidase in electropolymerized o-aminophenol film on platinized glassy carbon electrode. *Anal. Chem.* **1996**, *68*, 1632–1638. [[CrossRef](#)]
203. Hu, C.; Yang, D.P.; Zhu, F.; Jiang, F.; Shen, S.; Zhang, J. Enzyme-labeled Pt@BSA nanocomposite as a facile electrochemical biosensing interface for sensitive glucose determination. *ACS Appl. Mater. Interfaces* **2014**, *6*, 4170–4178. [[CrossRef](#)]
204. Shrivastava, K.; Monisha; Kant, T.; Karbhal, I.; Kurrey, R.; Sahu, B.; Sinha, D.; Patra, G.K.; Deb, M.K.; Pervez, S. Smartphone coupled with paper-based chemical sensor for on-site determination of iron(III) in environmental and biological samples. *Anal. Bioanal. Chem.* **2020**, *412*, 1573–1583. [[CrossRef](#)]
205. Shrivastava, K.; Patel, S.; Sinha, D.; Thakur, S.S.; Patle, T.K.; Kant, T.; Dewangan, K.; Satnami, M.L.; Nirmalkar, J.; Kumar, S. Colorimetric and smartphone-integrated paper device for on-site determination of arsenic (III) using sucrose modified gold nanoparticles as a nanoprobe. *Microchim. Acta* **2020**, *187*, 173. [[CrossRef](#)]

206. Ghosale, A.; Shankar, R.; Ganesan, V.; Shrivastava, K. Direct-Writing of Paper Based Conductive Track using Silver Nano-ink for Electroanalytical Application. *Electrochim. Acta* **2016**, *209*, 511–520. [[CrossRef](#)]
207. Ghosale, A.; Shrivastava, K.; Shankar, R.; Ganesan, V. Low-Cost Paper Electrode Fabricated by Direct Writing with Silver Nanoparticle-Based Ink for Detection of Hydrogen Peroxide in Wastewater. *Anal. Chem.* **2017**, *89*, 776–782. [[CrossRef](#)] [[PubMed](#)]
208. Kong, F.Y.; Gu, S.X.; Li, W.W.; Chen, T.T.; Xu, Q.; Wang, W. A paper disk equipped with graphene/polyaniline/Au nanoparticles/glucose oxidase biocomposite modified screen-printed electrode: Toward whole blood glucose determination. *Biosens. Bioelectron.* **2014**, *56*, 77–82. [[CrossRef](#)] [[PubMed](#)]
209. Li, W.; Qian, D.; Wang, Q.; Li, Y.; Bao, N.; Gu, H.; Yu, C. Fully-drawn origami paper analytical device for electrochemical detection of glucose. *Sens. Actuators B Chem.* **2016**, *231*, 230–238. [[CrossRef](#)]
210. Kant, T.; Shrivastava, K.; Tapadia, K.; Devi, R.; Ganesan, V.; Deb, M.K. Inkjet-printed paper-based electrochemical sensor with gold nano-ink for detection of glucose in blood serum. *New J. Chem.* **2021**, *45*, 8297–8305. [[CrossRef](#)]
211. El-Ads, E.H.; Galal, A.; Atta, N.F. Electrochemistry of glucose at gold nanoparticles modified graphite/SrPdO₃ electrode—Towards a novel non-enzymatic glucose sensor. *J. Electroanal. Chem.* **2015**, *749*, 42–52. [[CrossRef](#)]
212. Rafatmah, E.; Hemmateenejad, B. Dendrite gold nanostructures electrodeposited on paper fibers: Application to electrochemical non-enzymatic determination of glucose. *Sens. Actuators B Chem.* **2020**, *304*, 127335. [[CrossRef](#)]
213. Yang, M.; Liu, M.; Cheng, J.; Wang, H. A movable type bioelectronics printing technology for modular fabrication of biosensors. *Sci. Rep.* **2021**, *11*, 22323. [[CrossRef](#)]
214. Ghorbani, L.; Rabbani, M. Fabrication of a time-temperature indicator by inkjet printing of a spore-based bio-ink. *Bioprinting* **2021**, *21*, e00109. [[CrossRef](#)]
215. Kosmala, A.; Wright, R.; Zhang, Q.; Kirby, P. Synthesis of silver nano particles and fabrication of aqueous Ag inks for inkjet printing. *Mater. Chem. Phys.* **2011**, *129*, 1075–1080. [[CrossRef](#)]
216. Hiraoka, M.; Hasegawa, T.; Abe, Y.; Yamada, T.; Tokura, Y.; Yamochi, H.; Saito, G.; Akutagawa, T.; Nakamura, T. Ink-jet printing of organic metal electrodes using charge-transfer compounds. *Appl. Phys. Lett.* **2006**, *89*, 173504. [[CrossRef](#)]
217. Sun, T.X.; Jabbour, G.E. Combinatorial screening and optimization of luminescent materials and organic light-emitting devices. *MRS Bull.* **2002**, *113*, 231101. [[CrossRef](#)]
218. Trotter, M.; Juric, D.; Bagherian, Z.; Borst, N.; Gläser, K.; Meissner, T.; von Stetten, F.; Zimmermann, A. Inkjet-printing of nanoparticle gold and silver ink on cyclic olefin copolymer for DNA-sensing applications. *Sensors* **2020**, *20*, 1333. [[CrossRef](#)] [[PubMed](#)]
219. Singh, M.; Haverinen, H.M.; Dhagat, P.; Jabbour, G.E. Inkjet printing-process and its applications. *Adv. Mater.* **2010**, *22*, 673–685. [[CrossRef](#)]
220. Castrejón-Pita, J.R.; Baxter, W.R.S.; Morgan, J.; Temple, S.; Martin, G.D.; Hutchings, I.M. Future, opportunities and challenges of inkjet technologies. *At. Sprays* **2013**, *23*, 541–565. [[CrossRef](#)]
221. Colella, R.; Rivadeneyra, A.; Palma, A.J.; Tarricone, L.; Capitan-Vallvey, L.F.; Catarinucci, L.; Salmeron, J.F. Comparison of Fabrication Techniques for Flexible UHF RFID Tag Antennas [Wireless Corner]. *IEEE Antennas Propag. Mag.* **2017**, *59*, 159–168. [[CrossRef](#)]
222. Kumar, P.; Ebbens, S.; Zhao, X. Inkjet printing of mammalian cells—Theory and applications. *Bioprinting* **2021**, *23*, e00157. [[CrossRef](#)]
223. Sumaiya, S.; Kardel, K.; El-Shahat, A. Organic Solar Cell by Inkjet Printing—An Overview. *Technologies* **2017**, *5*, 53. [[CrossRef](#)]
224. Martin, G.D.; Hoath, S.D.; Hutchings, I.M. Inkjet printing—The physics of manipulating liquid jets and drops. *J. Phys. Conf. Ser.* **2008**, *105*, 012001. [[CrossRef](#)]
225. Noh, Y.Y.; Zhao, N.; Caironi, M.; Siringhaus, H. Downscaling of self-aligned, all-printed polymer thin-film transistors. *Nat. Nanotechnol.* **2007**, *2*, 784–789. [[CrossRef](#)]
226. Ko, H.Y.; Park, J.; Shin, H.; Moon, J. Rapid self-assembly of monodisperse colloidal spheres in an ink-jet printed droplet. *Chem. Mater.* **2004**, *16*, 4212–4215. [[CrossRef](#)]
227. Bartolo, D.; Boudaoud, A.; Narcy, G.; Bonn, D. Dynamics of non-newtonian droplets. *Phys. Rev. Lett.* **2007**, *99*, 174502. [[CrossRef](#)] [[PubMed](#)]
228. Park, J.U.; Hardy, M.; Kang, S.J.; Barton, K.; Adair, K.; Mukhopadhyay, D.K.; Lee, C.Y.; Strano, M.S.; Alleyne, A.G.; Georgiadis, J.G.; et al. High-resolution electrohydrodynamic jet printing. *Nat. Mater.* **2007**, *6*, 782–789. [[CrossRef](#)] [[PubMed](#)]
229. Ko, S.H.; Pan, H.; Grigoropoulos, C.P.; Luscombe, C.K.; Fréchet, J.M.J.; Poulidakos, D. All-inkjet-printed flexible electronics fabrication on a polymer substrate by low-temperature high-resolution selective laser sintering of metal nanoparticles. *Nanotechnology* **2007**, *18*, 345202. [[CrossRef](#)]
230. Son, Y.; Yeo, J.; Moon, H.; Lim, T.W.; Hong, S.; Nam, K.H.; Yoo, S.; Grigoropoulos, C.P.; Yang, D.Y.; Ko, S.H. Nanoscale electronics: Digital fabrication by direct femtosecond laser processing of metal nanoparticles. *Adv. Mater.* **2011**, *23*, 3176–3181. [[CrossRef](#)] [[PubMed](#)]
231. Soltman, D.; Subramanian, V. Inkjet-printed line morphologies and temperature control of the coffee ring effect. *Langmuir* **2008**, *24*, 2224–2231. [[CrossRef](#)]
232. Yu, X.; Xing, R.; Peng, Z.; Lin, Y.; Du, Z.; Ding, J.; Wang, L.; Han, Y. To inhibit coffee ring effect in inkjet printing of light-emitting polymer films by decreasing capillary force. *Chin. Chem. Lett.* **2019**, *30*, 135–138. [[CrossRef](#)]

233. Sliz, R.; Czajkowski, J.; Fabritius, T. Taming the Coffee Ring Effect: Enhanced Thermal Control as a Method for Thin-Film Nanopatterning. *Langmuir* **2020**, *36*, 9562–9570. [[CrossRef](#)]
234. Rodrigues, J.; Desai, S. The nanoscale Leidenfrost effect. *Nanoscale* **2019**, *11*, 12139–12151. [[CrossRef](#)]
235. Graddage, N.; Chu, T.Y.; Ding, H.; Py, C.; Dadvand, A.; Tao, Y. Inkjet printed thin and uniform dielectrics for capacitors and organic thin film transistors enabled by the coffee ring effect. *Org. Electron.* **2016**, *29*, 114–119. [[CrossRef](#)]
236. Lee, A.; Sudau, K.; Ahn, K.H.; Lee, S.J.; Willenbacher, N. Optimization of experimental parameters to suppress nozzle clogging in inkjet printing. *Ind. Eng. Chem. Res.* **2012**, *51*, 13195–13204. [[CrossRef](#)]
237. Derby, B. Inkjet printing of functional and structural materials: Fluid property requirements, feature stability, and resolution. *Annu. Rev. Mater. Res.* **2010**, *40*, 395–414. [[CrossRef](#)]